2019-01-01

# A Method For Iron Determination During Copper Electrometallurgy And Its Application To The Calculation Of Current Efficiency

Daniel Pedro Cruz
*University of Texas at El Paso*

# A METHOD FOR IRON DETERMINATION DURING COPPER ELECTROMETALLURGY AND ITS APPLICATION TO THE CALCULATION OF CURRENT EFFICIENCY

DANIEL PEDRO CRUZ

Master's Program in Metallurgical and Materials Engineering

APPROVED:

Guikuan Yue, Ph.D., Chair

Namsoo Kim, Ph.D.

Antonio Arribas, Ph.D.

Stephen L. Crites, Jr., Ph.D.
Dean of the Graduate School

To Micol and Laura, for their unconditional support

# A METHOD FOR IRON DETERMINATION DURING COPPER ELECTROMETALLURGY AND ITS APPLICATION TO THE CALCULATION OF CURRENT EFFICIENCY

by

DANIEL PEDRO CRUZ, B.S.

THESIS

Presented to the Faculty of the Graduate School of

The University of Texas at El Paso

in Partial Fulfillment

of the Requirements

for the Degree of

MASTER OF SCIENCE

Department of Metallurgical, Materials & Biomedical Engineering

THE UNIVERSITY OF TEXAS AT EL PASO

December 2019

## Abstract

With the objective of developing statistical models that describe iron kinetics under typical copper electrolytes as well as its effects on current efficiency and influence in cathodic and anodic behavior, a detailed electrochemical analysis is done in this work as a contribution to implement hydrometallurgical processes in the refining or winning process to produce high purity copper.

This thesis evaluates the oxidation-reduction potential (ORP) of the $Fe^{3+}/Fe^{2+}$ couple in the $H_2SO_4$-$Fe_2(SO_4)_3$-$FeSO_4$-$H_2O$ and $H_2SO_4$-$CuSO_4$-$Fe_2(SO_4)_3$-$FeSO_4$-$H_2O$ systems, with addition of different copper concentrations and temperatures up to 70°C, typically employed in the industry. This study further validates and expands a thermodynamic expression developed by Yue et al. to predict the redox potential of the $H_2SO_4$-$CuSO_4$-$Fe_2(SO_4)_3$-$FeSO_4$-$H_2O$ system. This expression establishes a mathematical relationship between temperature, $Fe^{3+}/Fe^{2+}$ ratio and ORP, and therefore provides an alternative way of the determination of ferric and ferrous concentration in the electrolyte based on the measurements of ORP and T. Furthermore, a model developed by Khouraibchia and Moats (2009,2010) [1, 2] to calculate current efficiency based on current density and concentrations of copper and ferric is employed in this work in an attempt to evaluate the current efficiency-ferric/ferrous concentration relationship.

Various sets of open circuit potential (OCP) tests were conducted to study the thermodynamic tendency of $Fe^{3+}/Fe^{2+}$ nominal ratio with temperature, copper concentration, acid concentration and iron concentration. Potentiometric determination of the ferrous iron was conducted to study the presence of iron ions and determine species in solution.

All electrochemical assays were carried out by preparing a synthetic solution utilizing a standard three-electrode cell to simulate a small-scale electrowinning cell and also, by expanding parameters, an electrorefining cell. Redox potential of the $Fe^{3+}/Fe^{2+}$ couple was measured via a

potentiostat/galvanostat VersaSTAT 3F and temperature was controlled with a PolySci circulating bath. Potentiometric titrations where carried out with an accumet ab200 pH/conductivity meter and a 50 ml burette for volumetric measurements.

Measured ORP results are in well agreement with the predicted ORP from developed equation at all nominal $Fe^{3+}/Fe^{2+}$ ratios and temperatures (25 to 70°C), with no more than ±3 mV difference. This confirm the validation of the model developed by Yue et al. by reliable prediction of measured redox potential based on 2 variables; nominal $Fe^{3+}/Fe^{2+}$ ratio and temperature.

The measured free $Fe^{2+}$ concentration by potentiometry showed an average percent error of 2.53% when compared to initial values and no observable relationship with temperature variation. This further validates the expression developed by Yue et al., qualitatively and quantitatively.

These findings expand the applicability of the equation to predict the redox potential in the $H_2SO_4$-$Fe_2(SO_4)_3$-$FeSO_4$-$H_2O$ and $H_2SO_4$-$CuSO_4$-$Fe_2(SO_4)_3$-$FeSO_4$-$H_2O$ systems and provide an alternative through this equation to avoid complicated speciation calculations and volumetric methods for ferric and ferrous determination.

The applicability of the equation in the current efficiency loss caused by iron in copper electrolytes was investigated using Eq. (2.12) for current efficiency. Results of the presumable current efficiencies obtained by using equation (2.12) showed several inconsistencies among CE values from the two industrial solutions (ER and EW) and consequently equation (2.7) couldn't be employed to establish a relation to the current efficiency factor. This is due to the lack of a complete set of data from each solution such as real ferric/ferrous ratio and ORP measurements.

Further industrial data will be investigated to support this method to apply Eq. (2.7) in iron determination and for the direct calculation of current efficiency.

# Table of Contents

## List of Figures

## List of Tables

## List of Illustrations

# 1 Introduction

## 1.1 Electrometallurgy of Copper

All copper recovered either for its production from ore, as well as recovered from scrap-recycle is treated by an electrochemical process. This allows access to high purity copper grade necessary for electrical applications (its most important and common application).

Copper sulfide minerals (0.5-2.0% Cu) are typically concentrated (20-30% Cu) and smelted to obtain a 50-70% Cu matte, from which then are electrorefined from impure copper anodes (99.5% Cu) to a final 99.99% copper cathode. Copper is recovered from oxide minerals (~0.5% Cu) under sulfuric acid leaching (~20% Cu) and sent via solvent extraction, where two immiscible liquids are mixed and then naturally separate, copper moves from one to the other, making a high Cu electrolyte to then be electrowon to a final 99.99% copper cathode (Figure 1). Electrorefining produces the majority of cathode copper 80% as opposed to 20% from electrowinning. Among copper ores, copper-iron-sulfide ores account for the majority of the world's copper-from-ore source, and the tendency is to develop a hydrometallurgical process for the treatment of these sulfides, a less energy consuming method, less harmful to the environment, and other potential advantages such as lower capital costs [1, 3, 4].

Chalcopyrite is the most abundant of these minerals, but is highly refractory to hydrometallurgical processing, resulting in the formation of an anodic passivation layer on the surface that renders the process kinetics very slow requiring potent solutions to dissolve it, and although pyrometallurgical processing remains as the principal industry method to treat chalcopyrite and the majority of sulfide ores, the high capital costs associated with smelting, the limited ability of smelters to handle growing concentrations of As and Sb, as well as emissions of

$SO_2$, lead efforts to implement a hydrometallurgical process to treat sulfide ores rather than improve their usual processing by the mining industry [1, 5, 6, 7].

According to Schlesinger et al. [1], copper production cost from electrowon cathodes (hydrometallurgical process) are significantly lower than copper produced by electrorefined cathodes (pyrometallurgical process), from $1 to $2 per kg to $3-$6 per kg, respectively.

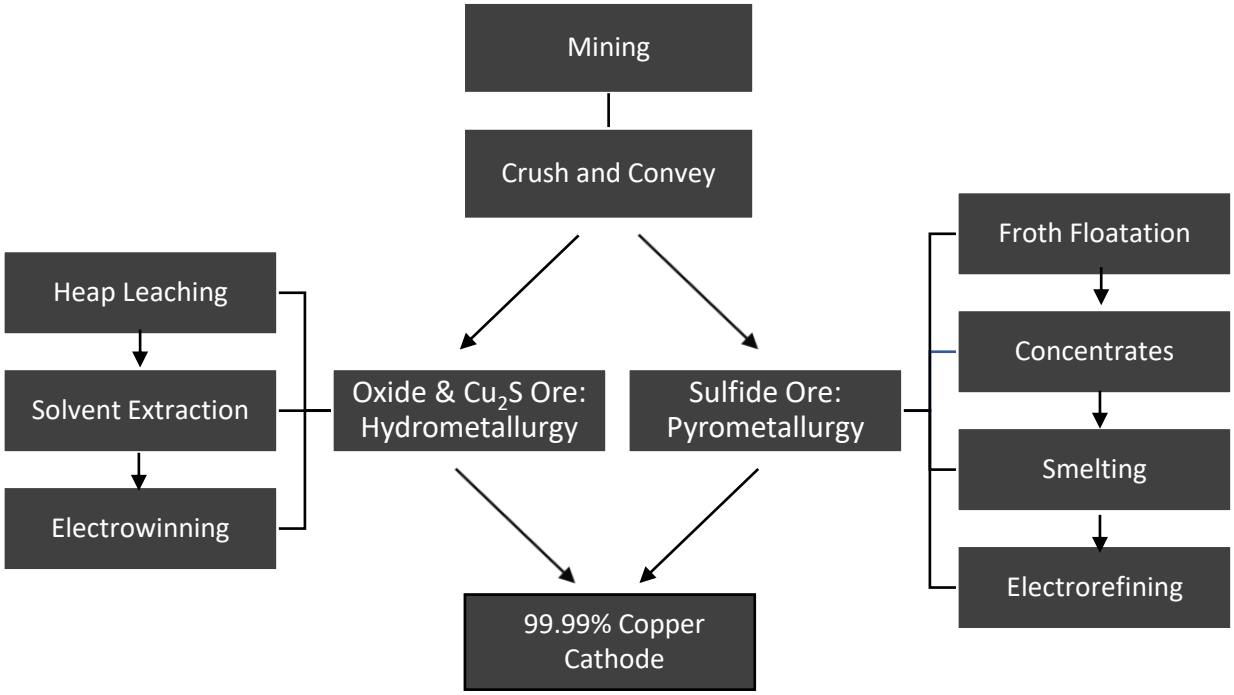


***Figure 1-1 Processing of Copper Ores***

## 1.2 Electrorefining of Copper

Electrorefining is employed to primary copper sulfide ores treated by a pyrometallurgy process shown in the right side of figure 1-1. These ores are highly refractory to acid treatments used in copper hydrometallurgy, less expensive and more hazardous to the environment. Copper recovered in the electrolyte comes from impure copper anodes (98.5-99.5% Cu), smelted and smothered almost free of sulfur and oxygen. The anodes are electrochemically dissolved in the electrolyte to produce 99.99% Cu, where impurities are lost during this anode-to-electrolyte-to-cathode passage, figure 1-2 [8, 9]. An electrical potential is applied to allow for this passage according to the following reactions:

$$Cu^0_{anode} \rightarrow Cu^{2+} + 2e \quad E^0 = -0.34\,V \tag{1.1}$$

$$Cu^{2+} + 2e^- \rightarrow Cu^0_{cathode} \quad E^0 = 0.34\,V \tag{1.2}$$

the cathode reaction is the reverse of that at the anode and therefore, in the ideal case, the cell voltage is only required to drive the current through the electrolyte, of around 0.3 V. A typical ER electrolyte contains 40 to 55 g/L of Cu in the form of $CuSO_4$ with a 300 to 400 kg anode and 170 to 200 g/L of $H_2SO_4$ (2M). Temperature is usually maintained at 60-65℃ (inlet to cell) to help increase the dissolution of copper sulfate, lower solution density and viscosity and increasing the rate of reactions [1, 9]. Electrolytes can vary significantly in impurity concentrations, (been Ni, As and Fe the higher in concentration with 10-20 g/L, 2-30 g/L and up to 3 g/L, respectively) depending on the composition of the incoming anodes, which depends in turn on the source of the smelter feed. Excessive current density causes increased impurity levels deposited in the cathode and also passivation of the anode due to a copper sulfate precipitation layer, created by the higher

oxidation rate of copper compared to cathode reduction of the ions, insulating the anode and restricting further oxidation of Cu to $Cu^{2+}$ [1, 16, 17, 53].

Increasing Cu(II) and sulfate contents enhance the formation of this passivation film. Passivation can also be promoted as more impurities are present in the anode and at higher concentrations (As, Ni, Sb, Sn, Pb) through the formation of a coherent slimes layer, as well as by the formation of a nickel sulfate film when high levels of nickel are present [1, 10, 11].

Typically, current densities below 300 $A/m^2$ are employed to avoid passivation, although newer developed methods allowed for densities to reach the 400 $A/m^2$ [1, 10, 11, 12]. Arsenic is the only known element to inhibit passivation, and is maintained at about 300 mg/L concentration in the anode [10]. According to literature [1, 9, 14, 15], the three main factors causing current inefficiencies are occasioned by stray currents to ground, anode-cathode short circuits and loss of copper deposit by air or $Fe^{3+}$ oxidation. Stray current loss is due to spilled electrolyte, causing 1 to 3% loss. Short-circuiting is caused by anodes and cathodes touching each other, around 1 to 3% loss and mostly due by nodular or dendritic growth that can be avoid by suitable addition agents and proper vertical placement of the electrodes. Oxygen and Fe(III) can reoxidized plated copper into the electrolyte causing around 1% loss according to the following reaction:

$$Cu^0 + 0.5O_2 + 2H^+ \rightarrow Cu^{2+} + H_2O \quad (1.3)$$

$$Cu^0 + 2Fe^{3+} \rightarrow Cu^{2+} + 2Fe^{2+} \quad (1.4)$$

Smooth and quiet flow of the electrolyte can avoid oxygen absorption to a certain point to still allow for mass transfer. The role of iron will be discussed further in the following chapters. Most refineries operate at current densities between 200 and 250 $A/m^2$.

Uniform electrode spacing, vertical hanging of anodes and cathodes, flat cathodes, good electrolyte composition and avoidance of passivation are all aimed at this requirement for uniform current distribution [15].

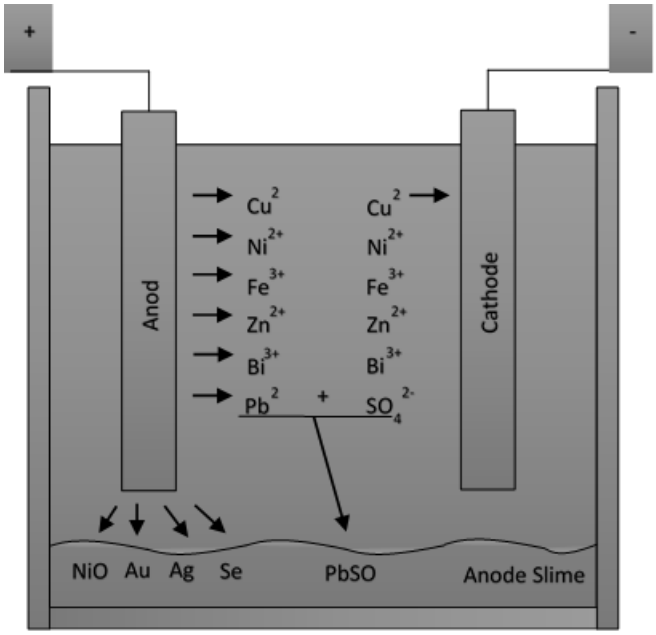


***Figure 1-2 Diagram of the electrolysis of copper from an impure anode (98-99.5% Cu anode) [53].***

Differing current density in a tankhouse can cause poor product copper quality (high local convection and slime contents), decreased current efficiency (higher energy consumption), local passivation and short circuits. In the other hand, there is always some oxygen evolution even with careful control of the electrical input to the cell, which not only reduces current efficiency but also causes an acid mist above the cells. This acid mist is primarily sulphuric acid health hazardous and needs to be minimized.

Electrorefining accounts for the 80% of high-purity copper production in the world, giving a copper cathode of less than 20 ppm impurities necessary for electrical applications. Research is

mostly focused in the understanding and improvement of the electrochemical reactions to achieve a better control of the electrolyte and further treat more complex anodes with higher concentrations of impurities and reduce operational cost by reducing power consumption, maximize copper cathode quality, and hopefully translate it to a more environmentally friendly hydrometallurgical process. Nevertheless, improvements have been made by developing new equipment and infrastructure as the use of polymer concrete cells, stainless steel cathodes and the implementation of automation in the tankhouse in an effort to improve the refining process as far as power consumption, productivity and waste reduction.

## 1.3 Electrowinning of Copper

Electrowinning is employed to primary copper oxide ores treated by a hydrometallurgy process as shown in the left side of figure 1-1. Copper is recovered onto a cathode from a purified electrolyte solution which will contain a range of impurities in the order of $10^{-3}$ ppm which can either be codeposited, precipitate or form slimes from the impure feed solution. The feed solution may be directly from a leach operation or may be partly or wholly purified prior to electrowinning.

A voltage from an external source is applied to the electrolyte containing $CuSO_4$ and $H_2SO_4$, causing current flow between the electrodes, anode to cathode, plating a purer metallic copper from the electrolyte onto the cathode, similar to the cathode reaction in electrorefining. In the anode, however, water is decomposed to release protons and form oxygen gas [1], different from the anode reaction in electrorefining.

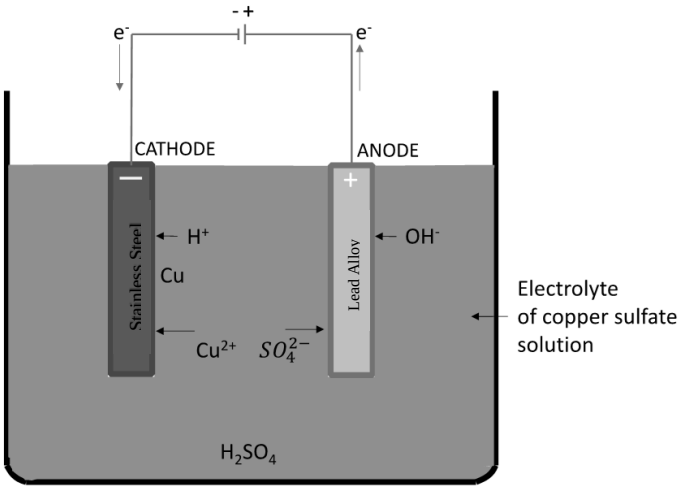


***Figure 1-3 Diagram of the electrolysis of copper from copper sulfate solution (inert anode).***

The cell voltage is around the 2.0 V according to current and voltage contributions to power consumption (approximately 2000 kWh/t) that can be found elsewhere in literature [1, 15, 16, 17]. Figure 1-3 shows a diagram of the electrolysis of copper using inert electrodes (electrowinning) where the negative cathode electrode attracts $Cu^{2+}$ ions (from copper sulfate) and $H^{+}$ ions (from water). Only the copper ion is discharged, being reduced to copper metal. The less reactive a metal, the more readily its ion is reduced on the electrode surface. Copper deposits forms as the positive copper ions are attracted to the negative electrode (cathode) (1.5), the negative cathode reaction. In the positive anode reaction, water is decomposed and oxygen evolution occurs (1.6). the sum of both reactions is the overall EW reaction (1.7).

$$Cu^{2+} + 2e \rightarrow Cu^{0} \qquad E^{0} = 0.34\ V \qquad (1.5)$$

$$H_2O - H^{+} + OH^{-} \rightarrow 0.5O_2 + 2H^{+} + 2e \qquad E^{0} = -1.23\ V \qquad (1.6)$$

$$H_2O \rightarrow H^{+}\ OH^{-} \rightarrow 0.5O_2 + 2H^{+} + 2e \qquad E^{0} = -0.89\ V \qquad (1.7)$$

The decomposition of water reaction at the anode produces oxygen gas ($O_2$), bubbling to the top generating an acid mist, and also contributes significantly to the overall cell voltage via required, 1.3 V of the 2.0 V. This mean that a decrease in the anode overpotential will reduce the cell voltage significantly, and thus decrease the total operating cost of the electrowinning process. A solution to this is the ferrous to ferric redox reaction, and will be covered in chapter 2.1.

Most of the currently proposed processes are based on sulfuric acid with ferric ions and/or dissolved oxygen as oxidants for leaching. Sulfuric acid is preferred over all other leaching reagents in terms of cost, environmental friendliness, and ease of its regeneration during electrowinning [1, 17, 18, 19].

Copper electrowinning is operated at current densities ranging from 150 to above 450 $A/m^2$, depending on electrolyte parameters and production needs. Higher currents can negatively affect the morphology and quality of the cathode. A typical electrolyte contains about 40 to 50 g/L Cu, 150 to 190 g/L of sulfuric acid ($H_2SO_4$), a temperature range of 45 to 60°C and a several iron concentrations based on nominal $Fe^{3+}/Fe^{2+}$ ratios, although concentrations are typically less than 3 g/L [1, 2, 17, 20, 21, 22, 23]. It is well known that iron reduces current efficiency in the electrolyte by around 3% for each 1 g/L of iron, due to the reduction of $Fe^{3+}$ ions to $Fe^{2+}$ at the cathode, stealing electrons to the copper reduction reaction. Iron behavior and effects on copper electrolytes will be further discussed in detail in chapter 2.1.1.

Manganese is also very important since in contributes to anode passivation in the electrolyte. Problems arising from manganese in the electrowinning electrolyte are known and a number of methods of control have been developed. Reducing manganese concentration in the electrolyte results in increased current efficiency and extended life of solvent extractant (SX) used in the solvent extraction electrowinning (SXEW) circuit [1, 20, 25].

To control the buildup of impurities in the electrolyte, as well as viscosity and oxygen dissolution, a bleed is performed regularly from the tankhouse, where part of it (around 50%) goes back to the SX for copper recovery. The reminder is discarded or goes back to the leaching process where the acid is reused.

Similarly, to electrorefining, inefficiencies in current are due by short circuits, stray current to ground, $Fe^{3+}$ reduction to $Fe^{2+}$, oxygen dissolution at the cathode, redissolution/oxidation of the copper cathode and electroplated copper falling off unable to be harvested.

## 1.4 Scope of Study

This thesis aims to contribute to the understanding of acidic iron sulfate solutions, prediction of redox potential of the $Fe^{3+}/Fe^{2+}$ couple in these solutions, and to quantify iron effect in copper electrometallurgy, both winning and refining.

Measured redox potentials in the Fe(II)-Fe(III)-$H_2SO_4$ and Fe(II)-Fe(III)-Cu(II)-$H_2SO_4$ systems at different temperatures and nominal $Fe^{3+}/Fe^{2+}$ will be compared to those calculated by the mathematical expression developed by Yue et al. [7, 18, 22, 26], to determine the validity of such equation and probably expand the scope of the same.

Potentiometric determination of ferrous iron will be conducted in order to revise solution concentration, analyze the $Fe^{3+}/Fe^{2+}$ behavior with temperature and to further validate the above expression.

Current efficiency will be evaluated in terms of cupric and ferric ions concentration in solution according to the equation developed by Khouraibchia et al. (2007) and will be validated based on currently used electrowinning and electrorefining industrial solutions.

These findings will enhance the investigation of anodic and cathodic behavior, assess the rate-determining steps involved in the electrolysis process, the possibility to expand the thermodynamic expression to predict the redox potential of the electrolyte, and finally contribute towards the expansion of hydrometallurgical processes.

# 2 Literature Review

## 2.1 Copper Electrolysis in the Fe(III)-Fe(II)-$H_2SO_4$-$H_2O$ System

By electrolysis, copper can be refined up to a 99.99% purity. Factors in the electrolyte such as acid concentration, temperature and current density must be selected so that both the anodic oxidation and the cathodic deposition of copper ions occur as efficiently as possible while impurities (other metals, complexes, etc.) are kept in the electrolyte to avoid their transfer from the anode to the cathode. These impurities either dissolve and accumulate in solution or fall to the bottom of the cell as anode slime. The build-up of impurities in solution is controlled by removing part of the electrolyte (a bleed) and removing the unwanted metals by precipitation or other means. The anode slimes are generally treated to recover valuable metals such as Ag, Au, Te and platinum-group metals [1, 20]. Additives are added to the electrolyte to enforce the correct behavior at both electrodes, to control copper electro-crystallization at the cathode (levelers and brighteners) and to help prevent insoluble particulates from co-deposition (surfactants).

It is well known that the influence of the acidic concentration (pH) is inversely proportional to the electrical conductivity (exchange current density) in the electrolyte, that is, a more acidic solution (low pH approximately $\geq 2$) propitiates a greater current density, beneficial for ion exchange[1, 7, 27]. This is true to a certain point, since high concentrations in the electrolyte can lead to anode passivation and higher viscosity, which results in increased solids in suspension and therefore reduced copper product quality via increased incorporation of impurity solids in the copper deposits. As can be seen, high current densities are desired in order to get more copper electroplated, yet quality of the cathode is compromised since more impurities can get trapped and plated between the copper, making a rougher surface.

Casas et al. (2005, 2006) developed a speciation model of the Fe(II)-Fe(III)-$H_2SO_4$- $H_2O$ system up to 1.3 M Fe and 2.2 M sulfuric acid concentration at 25 and 50℃. They observed a decrease in conductivity when temperature decreased and iron concentration increased, and a decrease in the concentration of $H^+$ and $Fe^{3+}$ as temperature increased. They also studied the dissolution of copper in acidic iron sulfate solutions and found that the dissolution rate showed a marked increase with both temperature and dissolved ferric iron. Dissolution rates were constant and then started to decrease as both $Fe^{3+}$ concentration and total copper surface area reduced gradually. Calculated free ferric ion species ($Fe^{3+}$) presented a very low concentration and the dominant Fe(III) specie was the $FeH(SO_4)_2$ neutral complex. The combined effect of increasing temperature and ferric iron concentration caused a marked increase in copper dissolution rates. These results indicate that the dissolution of the copper sheet was controlled mainly by the chemical reaction at the solid-liquid interphase.

Cifuentes et al. (2001, 2005, 2006) [21, 28, 29, 30] validated these model (Casas et al.) to determine the temperature dependence of the involved species' equilibrium constants and concentrations in Cu(II)-$H_2SO_4$ and Fe(II)-Fe(III)- $H_2SO_4$ at of 0-50 g/L Cu, 0-72.5 g/L Fe and 0-200 g/L $H_2SO_4$ concentrations for temperatures of 15 to 50℃. They further proved that these relationships can be used to predict Cu and Fe species concentrations with temperature in both systems and can also be used as components of more complex models.

The thermodynamic data of the main species involved (including $H^+$, $Fe^{2+}$, $Fe^{3+}$, $SO_4^{2-}$, $HSO_4^-$, $FeHSO_4^+$, $FeSO_4^0$, $FeHSO_4^{2+}$, $Fe(SO_4)^+$, $FeSO_4^+$, $Fe_2O_3$ and $H_2O$) have being studied by previous authors [6, 15, 18, 22, 26, 31] for the calculation of activity coefficients and equilibrium constants.

According to Yue et al [7], No precipitates are expected to be formed at temperatures from 25℃ to 70℃ under the specified conditions of a Cu liquor and so in this work, therefore will not

be considered. Acidities below pH 2 are typically employed, although higher acidity values will increase the electrolyte conductivity, they increase the corrosivity of the acid mist produced and decrease anode lifetime. Higher pH values will lead to the formation of iron precipitates and iron hydroxyl complexes [1, 7] Only species of significance to the scope of this experiment specified by the work of Yue et al. (2014, 2015) will be considered, according to the above mentioned functions of pH, temperature and nominal $Fe^{3+}/Fe^{2+}$.

### 2.1.1 Impurities in Copper Electrolysis

The behavior of the main impurities affecting copper electrolysis is governed by their position in the electrochemical series and will be discuss through all this work according to the process in which they are involved.

Generally, at the anode, elements with more positive reduction potentials (compared to copper) remain in solid form, while elements with less positive reduction potentials dissolve under the applied potential. At the cathode, elements with more positive reduction deposit preferentially, while elements with more negative potentials remain in solution [24]. Figures 2 and 3 show a comparison of the reduction potentials of main species present in electrowinning and electrorefining, respectively. As shown by these figures and according to literature, platinum and gold group metals, as well as selenium, tellurium, lead and tin do not dissolve in the electrolyte, instead they form slimes and fall to the bottom of the cell or adhere to the anode; in the other hand, arsenic, bismuth, cobalt, iron, nickel, sulfur and antimony do dissolve in the electrolyte under conditions where copper is electrochemically dissolved.

Elements that form slimes are recovered as biproduct and elements that do dissolve are bleed out of the electrolyte. Silver is more noble than Cu so it will be co-deposited at the cathode [(around 8-10 ppm according to Barrios, Alonso, & Meyer (1999)] yet is seen as a contribution rather than an impurity in deposited copper.

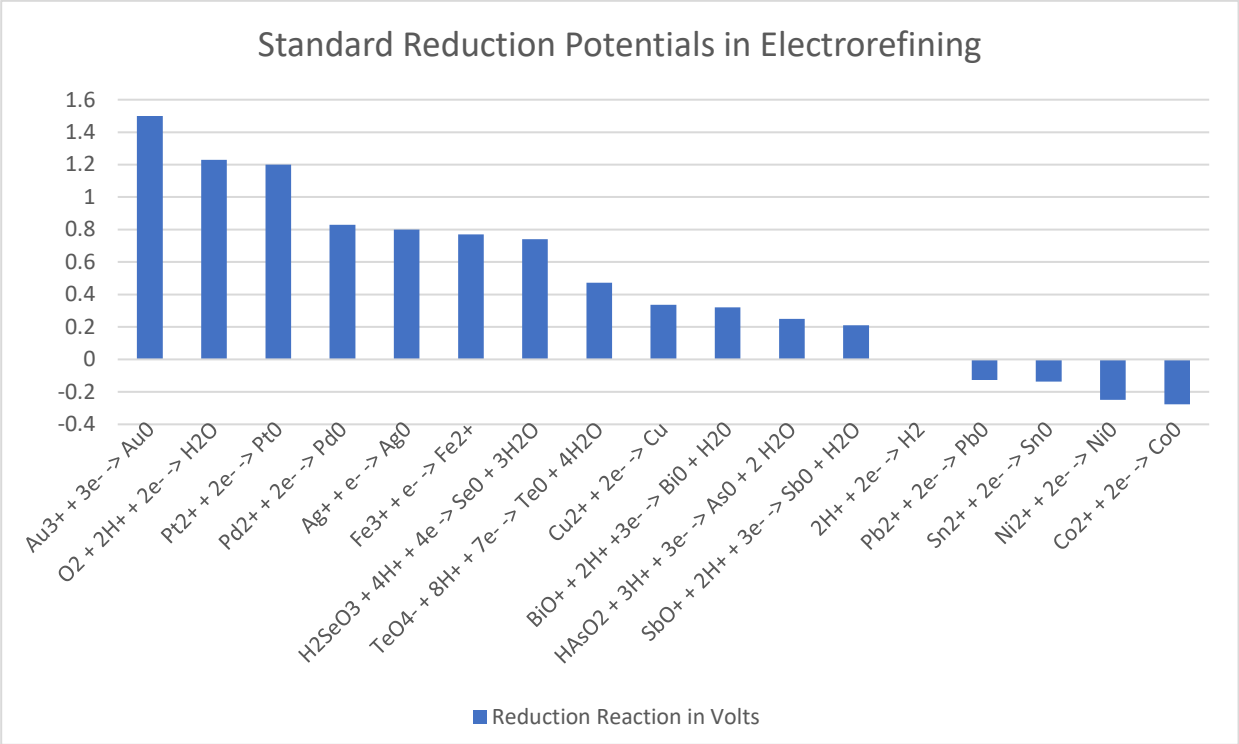


***Figure 2-1 Standard reduction potentials of the main species reactions involved in copper electrorefining***

During electro-wining, manganese is probably the second most important impurity for its detrimental contributions. It contributes to the formation of $MnO_2$ on the anode which can re-dissolve when power is lost, contributing to entrapment of Pb and Mn in the cathode and sludge formation at the bottom of the cell (Tjandrawan & Nicol. 2010) [1, 25]. Mn(II) can be oxidized to Mn(III), Mn(IV), or Mn(VII) at the anodes (Cheng, Hughes, Barnanrd, & Larcombe, 2000)[1, 5]. To avoid the formation of the permanganate ion ($MnO_4^-$) at the anode (highly oxidizing species that can have detrimental effects on the SX organic phase), a ratio of Fe:Mn in the electrolyte of approx. 10:1 is often maintained (miller 1995).

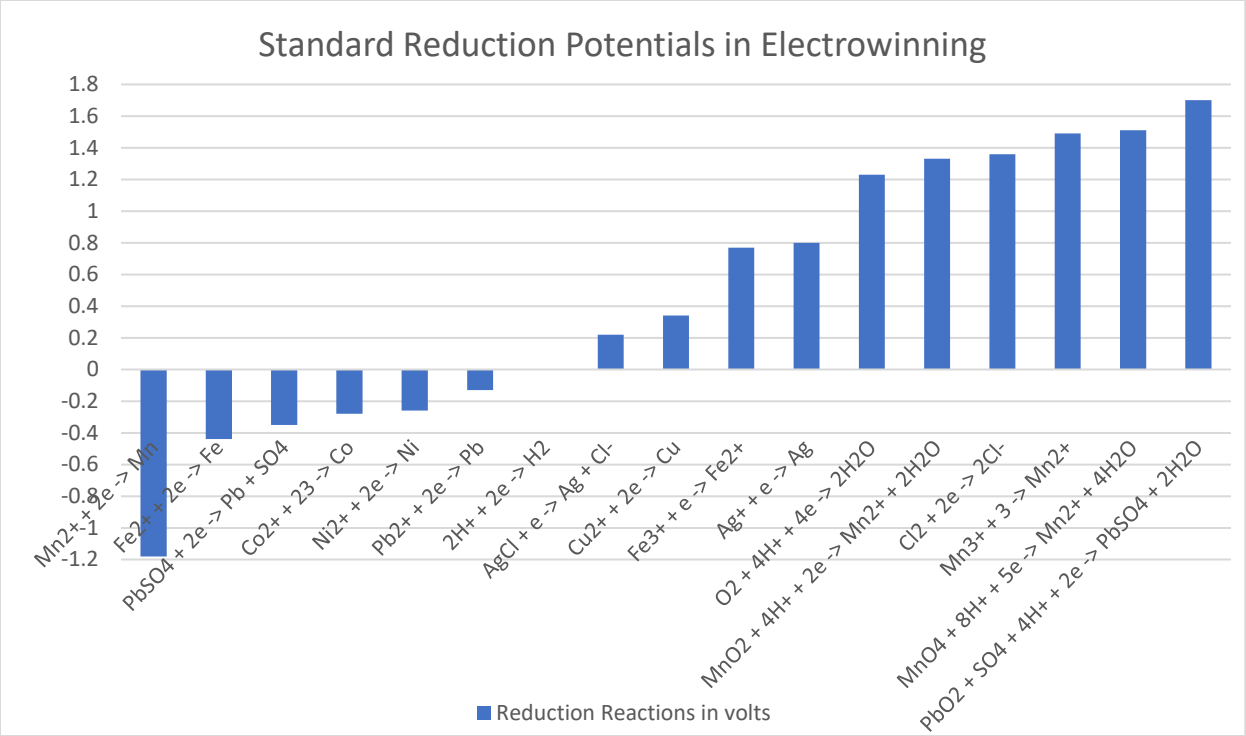


***Figure 2-2 Standard reduction potentials of the main species reactions involved in copper electrowinning***

### 2.1.2 The Iron Redox Reaction

It is well known that the iron couple is one of the most affecting elements in the electrolyte. At the cathode, the $Fe^{3+}$ to $Fe^{2+}$ reaction competes with the $Cu^{2+}$ to Cu reaction, which cause energy consumption of the cell to increase. It is also a rate-controlling factor in copper oxidation by the couple $Cu/Fe^{3+}$ to $Cu^{2+}/Fe^{2+}$ where the resulting $Fe^{2+}$ is reoxidized to $Fe^{3+}$ by $O_2$, where the redox couple $Fe^{3+}/Fe^{2+}$ acts as a catalyst.

The ferrous to ferric ion oxidation (2.1.1) has been chosen as an alternative to the anode water decomposition (2.2.2) in the design of new copper electrowinning cells because its use allows a drastic reduction in the cell voltage, from about 2 V to 1 V [32, 33, 34, 35].

$$Fe^{2+} \rightarrow Fe^{3+} + e \qquad E = 0.77\ V \qquad (2.1)$$

$$2H_2O \rightarrow O_2 + 4H^+ + 4e \qquad E = 1.23\ V \qquad (2.2)$$

where the cathode reaction and overall cell reaction are as follows, respectively:

$$Cu^{2+} + SO_4^{2-} + 2e \rightarrow Cu + SO_4^{2-} \qquad (2.3)$$

$$Cu^{2+} + SO_4^{2-} + 2Fe^{2+} \rightarrow Cu + 2Fe^{3+} + SO_4^{2-} \qquad (2.4)$$

where the ferric iron generated at the anode can be reduced back to ferrous by sulfur dioxide according to the following stoichiometry:

$$2Fe^{3+} + SO_2 + 2H_2O \rightarrow 2Fe^{2+} + 4H^+ + SO_4^{2-} \qquad (2.5)$$

In addition, this reaction eliminates the acid mist generated by oxygen 'bubbling' due to the water decomposition reaction, and the produced ferric ion can be used as an oxidizing agent. The oxidation of ferrous to ferric iron is a diffusion-controlled reaction, thus depends on the effective mass transport of both species for an effective voltage reduction to occur.

The use of iron, however, implies limitations in current densities due to the inability to obtain a sufficiently high rate of diffusion of ferrous iron to the anode and ferric iron from the anode, in other words, an optimum transport of ferrous and ferric ions is difficult to achieve.

Sandoval et al. (2005) [35], found that a flow-through anode and an effective circulation of the electrolyte enables a sufficient diffusion rate of ferrous iron to the anode and facilitate transport of ferric iron from the anode to achieve an overall cell voltage of less than about 1.5 V and current densities of 280 A/m$^2$, where the concentration of iron in the electrolyte is maintained between 10 to 60 g/L and temperature is between the 43 and 83°C. The redox potential of the above ferric-ferrous couple is given by the Nernst equation as follows:

$$E = E^0 - \frac{RT}{F} \ln \left\{ \frac{(Fe^{2+})}{(Fe^{3+})} \right\} \tag{2.6}$$

where E and E$^0$ are solution redox potential and redox potential when $Fe^{2+}$ and $Fe^{3+}$ are at unit activity, respectively; R is gas constant, T is absolute temperature, F is Faraday constant and {} represent the activity in solution. If the assumption is made, that the total concentration ratio, is equal to the activity ratio of the two species, then we can predict the redox potential of the solution by Nernst equation [18, 21]. The problem with the Nernst equation is that at higher electrolyte concentrations, the activity of any given species in solution cannot be related to its concentration in a simple way. If the ferrous/ferric activity ratio in any given solution were known, the Nernst

equation could be used to predict the solution redox potential. It can also be assumed that both ratios are proportional, and Nernst equation can be modified by a factor and even to a power of the total concentration, that is $\{Fe^{2+}\} / \{Fe^{3+}\} = a[Fe^{2+}] / [Fe^{3+}]$, where the firsts are activities and the last are concentrations.

Yue et al. developed an expression (2.7) to predict the redox potential of the $Fe^{3+}/Fe^{2+}$ couple depended only by the variables of temperature and nominal $Fe^{3+}/Fe^{2+}$ [7, 26]. According to Yue et al., the predicted potentials from this expression are in agreement with those found in literature, however further work is required to expand the range of application of this expression.

$$E(mV) = -1 \times 10^{-3} \times [T(K)]^2 + 0.91 \times T(K) + \frac{2.303R}{nF} \times T(K) \times 10^3 \times log \frac{C_{ferric,nominal}}{C_{ferrous,nominal}} + 492 \qquad (2.7)$$

It is the intention of the authors of this expression to avoid or skip the use of difficult calculations such as the Debye-Huckel and B-dot models for the estimation of activities and ionic strengths, and also to not need to employ chemistry analysis techniques that are quite difficult to carry on, inaccurate if not done correctly and very expensive in general.

## 2.2 Influence of Kinetics on Cell Efficiency

### 2.2.1 Current Efficiency

The exchange current density between electrodes can either accelerate or inhibit charge transfer [15]. These effects are complex combinations of thermodynamic and kinetic factors. The rate of copper plating from the solution is given by Faraday's Law;

$$m = MIt\xi/nF \tag{2.8}$$

where m is the mass of copper plated in grams, M is the molar mass of copper (63.55 g/mol), I is the current in the electrolyte in amperes, t is the time for which the current is applied in seconds, $\xi$ is the current efficiency (the fraction of the total current used in producing copper), n is the number of electrons involved in the plating of Cu (2 from the cathode reaction) and F is the Faraday constant (96 485 C/mol of charge = 96 485 A/mol).

Current density is directly proportional to electroplating, that is, the rate of plating increase with increase of current density. However, excessive current density can promote rough, nodular cathode deposits, and decreased copper purity if not properly managed [15, 16]. Current density in modern plants varies from 200 to 500 A/m$^2$, By Faraday's Law we can calculate the maximum amount of copper that can be plated in a given time period. The weight of the cathode is a function of the amount of current applied. More current (electrons) means more copper can be plated.

$$W_{cathode} = \frac{i \cdot A \cdot t \cdot a.w.}{n \cdot F} \tag{2.9}$$

where $W_{\text{cathode}}$ is the weight of the electroplated cathode in grams; $i$ is the current density in Amps per meter square; $A$ is the area available for plating in meter square; $t$ is plating time in seconds;

*a.w.* is the atomic weight of copper in g/mol (63.54 g/mol); *n* is the number of electrons and *F* is Faraday's constant in C/mol $e^-$ (96487 C/mol $e^-$).

Faradays' Law represents the maximum amount of copper that can be plated for a specified time period and current. Inefficiencies as iron ions, short circuits and stray current in the process result in less copper being plated than theoretically possible. To account for these inefficiencies a factor is applied to estimate how much copper is actually plated at a given operating conditions. The factor is called current efficiency (CE) and is represented as a percentage of theoretical performance:

$$W_{actual} = C.E.(W_{theoretical}) \tag{2.10}$$

where copper ER operations generally operate above 90% current efficiency and copper EW operations usually run about 80% current efficiency.

In the other hand, the open-circuit potential (OCP) in an electrochemical cell can be defined as the voltage measured when no current flows through the cell, or more technically it reflects the thermodynamic parameter which guides us about the thermodynamic tendency of that metallic materials to participate in the electrochemical corrosion with the electrolyte or neighboring medium. Therefore, a potential below OCP is more thermodynamically stable (less tendency to take part in corrosion) whereas the potential above OCP is considered as thermodynamically unstable and prone to corrosion.

Aslin et al. [36] studied the importance of even current densities as modern refineries approach their limiting current density as they employ higher current densities (<250 $A/m^2$). The maximum current density possible is related to the ability of cupric ions to migrate to the cathode surface as quickly as those ions can discharge from the anode. This is driven by the diffusion rate of cupric ions across the boundary layer at the cathode face. The thickness of the boundary layer

depends on many factors including flow rate of the bulk electrolyte and the concentration gradient across the boundary layer, as described by Fick's Law [10, 14, 28, 34, 37].

If the current density exceeds the ability of cupric ions to diffuse across the boundary layer the current will be carried by cations other than copper, and a reaction other than copper reduction at the cathode will occur. The limiting current density can be written as the equation;

$$i_{lim} = \frac{nFDC_b}{d} \tag{2.11}$$

where *i* is the current density (A/m$^2$), F is Faraday constant (C/mol) and *n* the number of moles of electrons in the electrochemical reaction. Electrode spacing, alignment, geometry, contact and internal resistance are contributors of non-uniform current distribution, yet electrolyte resistance is by far the biggest (80-85%).

Das and Krishna [37] showed an increase of every g per L will cause an increase in energy consumption from 1690 to 1827 kWh/t. Energy consumption increased when increased iron concentration from 0 to 6 g/L, within an average increase of 39 kWh/t for each addition of 1 g per L. the cell voltage was not dependent on iron concentration and has an average of 1.433 V with a standard deviation of 0,010. E.C. therefore increase was mainly caused by the decrease in current efficiency.

Khouraibchia et al. [1, 2] presented the first steps in developing a definitive relationship (2.12) for the 2 to 3% loss in current efficiency per every gram in a liter of a typical copper electrowinning electrolyte based on the diffusivity of ferric ions as a function of concentrations and temperature.

$$\xi(\%) = 88.19 - 4.91[Fe^{3+}] + 0.52[Cu^{2+}] + 1.81 \times 10^{-3} j - 6.83 \times 10^{-3}[Cu^{2+}]^2 + 0.028[Fe^{3+}][Cu^{2+}] + 4.015 \times 10^{-3} j[Fe^{3+}] \quad (2.12)$$

The authors used the Nernst diffusion layer model (Vetter, 1967) for the relationship between Fe(III) limiting current density and its diffusivity:

$$i_L = F \frac{D_{Fe(III)}}{\delta} C \quad (2.13)$$

where C is Fe(III) concentration (mol/cm$^3$); $D_{Fe(III)}$ is Fe(III) effective diffusivity (cm$^2$/s); $i_L$ is the limiting current density of the reduction of Fe(III) (A/cm$^2$); δ is the thickness of the Nernst diffusion boundary layer (cm); and F is the Faraday's constant = 96485 C/(e) mole. Their results showed current efficiency decrease linearly with increasing Fe, from 98.6 to 83.8% (0 to 6g/L). The slope indicates a 2.5% C.E. decrease for each addition of 1 g/L.

This model demonstrates that the current efficiency of the system is determined by the concentration of copper and ferric ions in the electrolyte, while current density does not have a significant effect. This model is used in this work to evaluate current efficiency as a function of $Fe^{3+}$ and $Cu^{2+}$ concentrations.

### 2.2.2 Cathode Quality

The operating parameters such as pH, current density and temperature during the electrolysis/electroplating process will determine the morphology and crystallographic structure of the metal deposits, which in turn will 'shape' the specific properties of the metal. Furthermore, the morphology and crystallographic structure of these deposits are mainly determined by the nucleation and growth of the grains, where the concentration of the solution is proportional to the nucleation rate and overpotential (Rate of Nucleation $\propto$ Conc of Ad-atoms $\propto$ Overpotential) [15]. Growth can be inhibited by the addition of various levelling or brightening agents which absorb preferentially on the crystal defects (the growth sites) [1, 5, 15, 34, 38].

Among the mentioned parameters affecting cathode quality, current density is the most significant regarding cathode's physical properties. The effect of current density on the morphology is shown in Figure 2-4 [15]. As expressed by Nicol et al., as the current density (or more accurately the ratio $i/i_L$) increases, the mean size of the crystallites making up the deposit decreases with well-formed large crystals giving way eventually to very fine crystals or powdery deposits. This is expected in terms of the effect of overpotential on the relative rates of nucleation and growth.

The maximum current density that can be applied in industrial operations is normally about 30-40% of the limiting current density. In the case of base metal electrowinning, a rule of thumb is that the ratio, current density ($A/m^2$) / metal concentration (g/L) in spent < 10 thus, for a cell concentration of 40 g/L Cu, the maximum current density should be about 400 $A/m^2$.

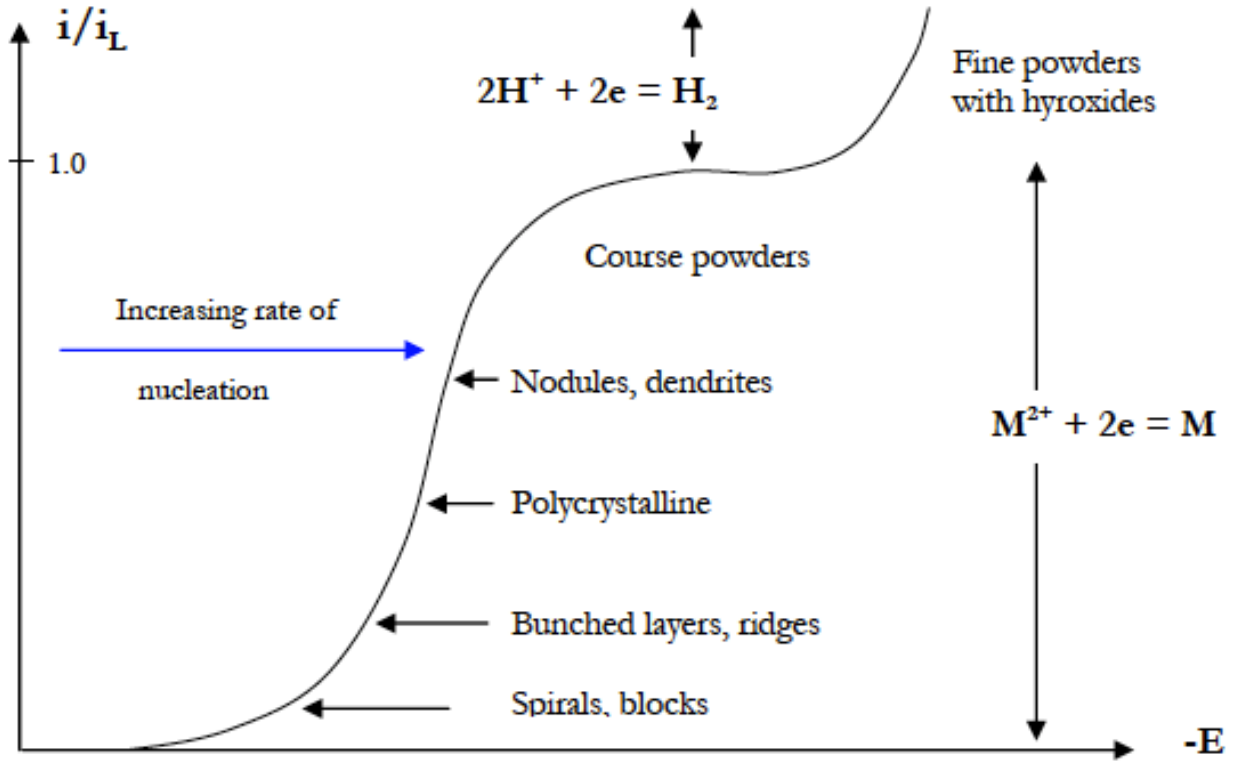


***Figure 2-3 Effect of current density on the nature of deposits. Electrowinning and Electrorefining of Copper, J. Nicol, Murdoch University***

The use of brighteners, levelers, inhibitors, and the chlorides are meant to improve the electrochemistry, structure, properties and appearance of electrodeposited copper [1, 37].

Brighteners are typically incorporated into the copper deposits and tend to refine the grain structure by catalyzing the copper reaction and promoting the formation of new grains. Levelers help produce a smooth surface by inhibiting the growth of protrusions or edges. Levelers and brighteners usually work well in conjunction with each other. Inhibitors are believed to affect both copper dissolution and deposition. They are described as polarizers or current suppressors. These additives have been shown to interact with the cathode surface and influence plating. They also produce deposits with tighter grain structures.

Chloride ions promote dense, fine grain, low impurity copper cathodes, but the concentration should be maintained below about 30 mg/L, since at higher concentration chlorine gas will be evolved at the anodes and pitting of the stainless steel cathodes is observed. Chloride ions are not only known to depolarize or accelerate the copper-plating process but also assist in interactions between the copper surface and suppressors (Shao, Pattanaik and Zangari, 2007). Thus, refineries control the addition of each of these compounds to obtain copper cathodes of desired quality and density. These compounds can also affect anode passivation in copper electrorefining (Moats and Hiskey, 2000).

## 2.3 Determination of Iron Species in Sulfuric Acid Solutions

To select an analytical method intelligently it is necessary to describe the chemical interactions between the components, know how much sample is available and the concentration range of the analyte (how sensitive the method must be accommodated), what components of the sample might cause interference (selectivity of the method), as well as the chemical properties of the sample matrix (solvent). Factors such as temperature and pH must also be accounted.

Iron speciation can be performed by titration, complexation, photochromatography, spectroscopically, and by a combination of spectrophotometry with the above mentioned. Volumetric spectroscopy techniques can be used effectively if several assumptions are made as mentioned in the last section, where the concentration of species is related to activities in an equally, proportional or exponentially manner.

Zhu et al. 2018 [40], modified the very well known spectophotometric method of 1,10-phenanthroline, preferred among other similar methods due to its sensitivity [Tong et al. 2016; Amonette and Matyas 2016; Sumitomo et al. 2017] to account for the interference that high concentrations of $Fe^{3+}$ causes to analyze $Fe^{2+}$. In the study, they masked $Fe^{3+}$ with $F^{-}$ (sodium fluoride) with a specific molar concentration, ratio but according to Tamura et al., (1974) [41] the masking with fluoride is only effective if the solution is maintained at low pH levels (below 2.5) to inhibit the interference of fluoride of accelerating the aerial oxidation of Fe (II). It also appears that temperature has no effect up to 30℃, yet since we pretend to explore temperatures up to the 70℃ this method becomes negligible for the purposes of this research.

A method proposed by Gendel et al. [4] in which Fe(III) and Fe(II) in concentration ratios of about 100:1 are first separated in solution in a pretreatment and then Fe(II) is determined by a modified phenanthroline method appears to be precise but very complicated compared to other available methods.

Titrations are among the most accurate of all analytical procedures. To mark the end point of a titration, an indicator is added to the analyte. Usually the amount of titrant is varied until chemical equivalence is reached, as indicated by the color change of a chemical indicator or by the change in an instrument response. The amount of the standardized reagent needed to achieve chemical equivalence can then be related to the amount of analyte present, thus, a type of chemical comparison.

Two strong oxidants are preferred over other methods to titrate iron, potassium permanganate ($KMnO_4$) and cerium ($Ce^{4+}$). Potassium dichromate ($K_2Cr_2O_7$) is somehow below these two and Iodine ($I_3^-$) as well as bromine ($KBrO_3$) are considered weak oxidants therefore are of no interest.

The permanganate end point is not permanent because excess permanganate ions react slowly with the relatively large concentration of Manganese(II) ion present at the end point, according to the reaction: $2MnO_4^- + 3Mn^2 + 2H_2O \rightleftharpoons 5MnO_2(s) + 4H^+$ with an equilibrium constant ($K_{eq}$) of $10^{47}$. If the solution is very dilute, diphenylamine sulfonic acid or the 1,10-phenanthroline complex of iron (II) provides a sharper end point [1, 2]. Solutions of Cerium(IV) are yellow-orange, but the color is not intense enough to act as an indicator in titrations, the most widely used is 1,10-phenanthroline or one of its substituted derivatives.

# 3 Objectives

The overall objective of this investigation is to determine iron behavior in copper electrowinning and electrorefining electrolytes. This is an effort to contribute to the investigation of published research to understand the current efficiency loss caused by iron.

In view of the preceding discussion, the specific objectives of this thesis are set out as follows:

(1) Conduct a simulation of the quaternary acidic sulfate solution [$H_2SO_4$-$Fe_2(SO_4)_3$-$FeSO_4$-$H_2O$] and a small-scale copper electrolyte solution [$H_2SO_4$-$CuSO_4$-$Fe_2(SO_4)_3$-$FeSO_4$-$H_2O$] to predict the oxidation-reduction potential of the $Fe^{3+}/Fe^{2+}$ couple in solution from 25℃ to 70℃ from Yue et al. thermodynamic model.

(2) Determine iron species concentrations in the $H_2SO_4$-$Fe_2(SO_4)_3$-$FeSO_4$-$H_2O$ and the $H_2SO_4$-$CuSO_4$-$Fe_2(SO_4)_3$-$FeSO_4$-$H_2O$ systems by potentiometric titration to validate the applicability of the model developed by Yue et al. to determine ferrous and ferric concentrations based on measured redox potential.

(3) To validate the thermodynamic model developed by Yue et al. on the prediction of the redox potential in the quaternary acidic iron copper sulfate solution and further extend its applicability to a broader range of pH, temperature, ferric/ferrous ratio, and concentrations of copper and iron ions.

(4) To expand the applicability of the equation to predict the redox potential in the $H_2SO_4$-$Fe_2(SO_4)_3$-$FeSO_4$-$H_2O$ and $H_2SO_4$-$CuSO_4$-$Fe_2(SO_4)_3$-$FeSO_4$-$H_2O$ systems and provide an alternative through this equation to avoid complicated speciation calculations and volumetric methods for ferric and ferrous determination.

# 4 Methodology and Experimental Procedure

## 4.1 Measurements of the Oxidation-Reduction Potential of the $H_2SO_4$-$Fe_2(SO)_3$-$FeSO_4$-$H_2O$ and the $H_2SO_4$-$CuSO_4$-$Fe_2(SO_4)_3$-$FeSO_4$-$H_2O$ Systems from 25℃ to 70℃

Experimental work to measure the redox potential of the quaternary acidic iron sulfate system was carried out at temperatures ranging from 25℃ to 70℃.

### 4.1.1 Electrolyte preparation

The composition of the synthetic iron containing solutions was determined based on industrial operating conditions during copper electrowinning and electrorefining. The total iron and copper concentrations ranged from 2.2 g/L to 6 g/L and 36 g/L to 50 g/L, respectively.

Deionized water, sulfuric acid ($H_2SO_4$, 95.0-98.0%, Fisher Scientific), iron (III) sulfate pentahydrate ($Fe_2(SO_4)_3$•$5H_2O$, 97%, Acros), iron (II) sulfate heptahydrate ($FeSO_4$•$7H_2O$, 99+% Acros) and copper (II) sulfate pentahydrate ($CuSO_4$•$5H_2O$, 98%, Acros) were used to prepare the electrolyte. Solution was prepared prior to each test, with $H_2SO_4$ concentrations ranging from 170 to 200 g/L, chosen to cover most of the current industrial processes. Ferric to ferrous concentration was set by various nominal ratios (1:100, 1:10, 1:5, 1:2, 1:1, 2:1, 5:1, 10:1, 100:1) in the range of total iron and copper concentrations above mentioned.

### 4.1.2 Electrode preparation

A platinum (inert) electrode is used in this work to reflect the chemical equilibrium of the reversible (redox) reaction in the $H_2SO_4$-$Fe_2(SO_4)_3$-$FeSO_4$-$H_2O$ system, where a high potential is indication of an oxidizing reaction and a low potential indicates a reduction reaction. A Pt electrode is chosen for its wide applicability according to literature [8, 18, 19, 20, 38, 39]. The platinum wire used is a 0.5 mm diameter, 99.9% (mass) Sigma-Aldrich wire. The wire was connected to a standard copper wire through a MG Chemicals silver conductive epoxy and protected from the sulfate solution by mounting it in an epoxy resin (832HT-375ML) from MG Chemicals, leaving a needle-like tip portion of the Pt wire exposed to the solution. The Pt working electrode was activated in a 0.1M $H_2SO_4$ solution according to published method (Zoski et al. 2007).

### 4.1.3 Silver Silver/Chloride saturated reference electrode

A reference electrode has a known defined potential, known as half-cell potential and is independent and completely insensitive of the electrolyte composition potential and little change with temperature. A saturated Ag/AgCl reference electrode was chosen in this work as reference in reduction potential measurements for its environmental advantages over the saturated calomel electrode. The electrode functions as a redox electrode and the equilibrium is between the silver and its salt silver chloride. It was fabricated using an Accumet glass body Ag/AgCl electrode with a glass salt bridge tube connected to a Luggin capillary, in which the electrode is a silver wire coated with a thin layer of silver chloride, with a porous end that allows contact between he field environment with the silver chloride electrolyte. The electrode body contains saturated potassium chloride solution to stabilize the silver chloride concentration.

### 4.1.4 Electrochemical measurements at 25℃, 35℃, 45℃, 55℃, 60℃, 65℃ and 70℃

Electrochemical tests were conducted using a standard three-electrode cell with a circulating bath for temperature control. An 8mm graphite rod served as counter electrode (CE), the Pt electrode as the working electrode (WE) and the Ag/AgCl electrode as the reference electrode. All potentials have been converted from Ag/AgCl to the standard hydrogen electrode (SHE) and all further potentials in this work are quoted with respect to SHE at 25℃ unless otherwise stated. Corrections used for the measured potential can be found in previous publications (Yue, 2015; Yue, Zhao, Olvera & Asselin, 2014). Temperature in the electrolyte was increased by a circulating bath from PolyScience and kept at constant temperature with a ±1℃ accuracy. The solution was deaerated by sparging argon or nitrogen prior and throughout the experiment at a constant flow rate to eliminated atmosphere oxidation (dissolved oxygen). The open circuit potentials (OCP) of the assays were recorded to yield a steady-state potential (as the redox-potential). A VersaSTAT 3F potentiostat/galvanostat controlled by a VersaStudio electrochemistry software (Princeton Applied Research) was used to measure and record all ORP-OCP values.

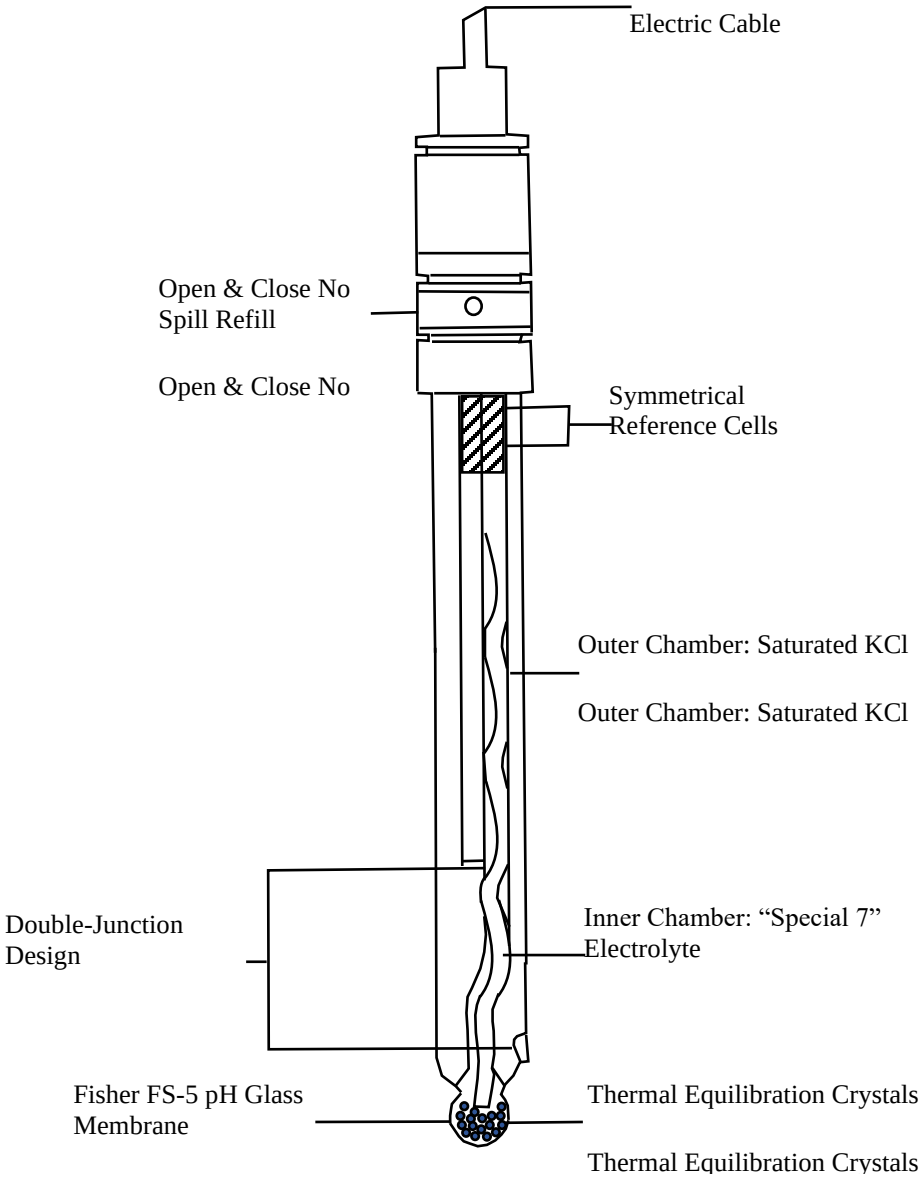


***Figure 4-1 Schematic of an Ag/AgCl combination reference electrode***

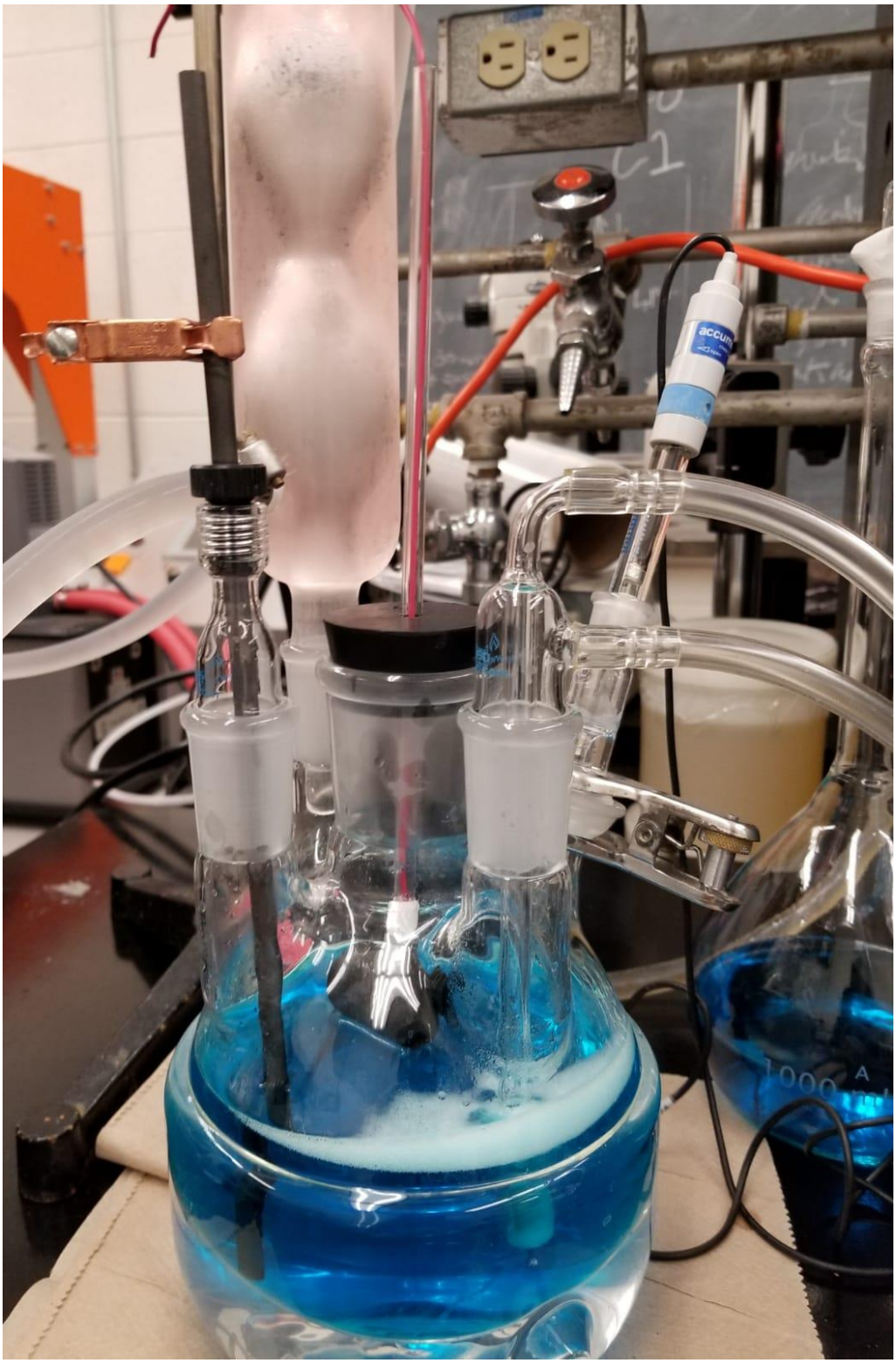

***Illustration 4 - 1 Set up of the ORP test of the $H_2SO_4$-$CuSO_4$-$Fe_2(SO_4)_3$-$FeSO_4$-$H_2O$ system in a standard 3-electrode cell***

### 4.1.5 Correction of the measured potentials to SHE at 25℃

The potential of the Ag/AgCl electrode depends on the concentration of the solution used in the electrode itself, in this case a saturated solution (KCl) where the potential is +0.197V and the SHE potential is a function of temperature and is zero only at 25℃ (based on the pH of the electrolyte) rather than zero at any temperature as is typically assumed. The measured redox potentials are corrected following the previous method mentioned (Yue, 2015; Yue, Zhao, Olvera & Asselin, 2014) and compared to the redox potentials E (mV) calculated by this equation in reference to SHE at 25℃ by the following equations:

$$E_{SHE}(T) = E_{obs} + E_{correction} = E_{obs} + E_{\frac{Ag}{AgCl}}(T) - \Delta E_{th} \tag{4.1}$$

$$E_{SHE}(25℃) = E_{SHE}(T) + \Delta E_{SHE} \tag{4.2}$$

where $E_{\mathrm{SHE}}$ (T) is the potential of the working electrode vs SHE at the operating temperature T; $E_{\mathrm{obs}}$ is the observed potential of the working electrode vs the external Ag/AgCl reference electrode filled with 0.1M KCl; $E_{\mathrm{correction}}$ is the potential correction value; $E_{\mathrm{Ag/AgCl}}$ (T) is the isothermal potential of the Ag/AgCl electrode vs SHE at operating temperature T and $\Delta E_{\mathrm{th}}$ is the measured potential difference of the thermal cell between an internal and external reference electrode connected by a cooled salt bridge. Since ΔEth values are highly related to temperature difference and relatively independent of different chloride-containing alkaline and neutral solutions with various concentrations, as reported by Bosch et al (2003) [2, 43], Δ*E*th was determined by the data published in the literature for 0.1 mol/kg KCl solution, with the values of about 15 mV at 70°C and 20 mV at 90°C, respectively.

This assumption is reasonable and it was verified by measuring the potential for an acid iron sulfate solution with the Cortest external Ag/AgCl RE filled with 0.1 mol/kg KCl. Δ*E*SHE was also calculated, with a value of 26.7 mV at 70°C and 36.1 mV at 90°C. It should be noted that the thermodynamic data of H2 used to calculate the Δ*E*SHE were obtained from the literature [2, 44, 45].

## 4.2 Measurements of the Potentiometric Determination of Iron(II) Ions with Cerium(IV) in the $H_2SO_4$-$Fe_2(SO_4)_3$-$FeSO_4$-$H_2O$ and the $H_2SO_4$-$CuSO_4$-$Fe_2(SO_4)_3$-$FeSO_4$-$H_2O$ Systems from 25°C to 70°C

Experimental work to quantify ferrous ions concentration in the electrolyte by potentiometric titration with cerium (IV) sulfate from room temperature up to 70 Celsius degrees.

### 4.2.1 Electrolyte Preparation

Titration was performed in 150 ml of each electrolyte prepared as described in previous chapter (4.1.1), titrating 25 ml of solution at each temperature (25, 35, 45, 55, 60 ,65 and 70°C). Please notice that liquors varied in concentrations of iron and copper and nominal $Fe^{3+}/Fe^{2+}$ ratios.

### 4.2.2 Titrant Preparation

Cerium (IV) sulfate ($Ce[SO_4]_2$) was prepared based on iron(II) concentration range of the electrolyte to accommodate for the sensitivity of the method. Deionized water, sulfuric acid ($H_2SO_4$, 95.0-98.0%, Fisher Scientific) and cerium (IV) sulfate tetrahydrate ($Ce(SO_4)_2 \cdot 4H_2O$, 98%, Acros) were used to prepare the titrant solution. Solution was prepared prior to each test according to ferrous to ferric ratio; the concentration of $Ce^{2+}$ was 0.01M in the 100:1 ratio, 0.1M in the majority of nominal ratios, and 1M concentration in 1:100, 1:10 and 1:5 ratios.

### 4.2.3 Electrochemical and Volumetric Measurements to Determine Real $Fe^{2+}$ Concentration in the $H_2SO_4$-$Fe_2(SO_4)_3$-$FeSO_4$-$H_2O$ and $H_2SO_4$-$CuSO_4$-$Fe_2(SO_4)_3$-$FeSO_4$-$H_2O$ systems at 25, 35, 45, 55, 60, 65 and 70℃

Electrochemical tests were carried out using a 50 ml jacketed beaker for temperature control. An accumet Pt pin Ag/AgCl (FisherScientific) combination (pH/ORP) electrode was used to measure the redox potential of the electrolyte during the gradual addition of Cerium (IV) with the help of a standard volumetric burette to the 25 ml electrolyte ash shown in illustration 4-2.

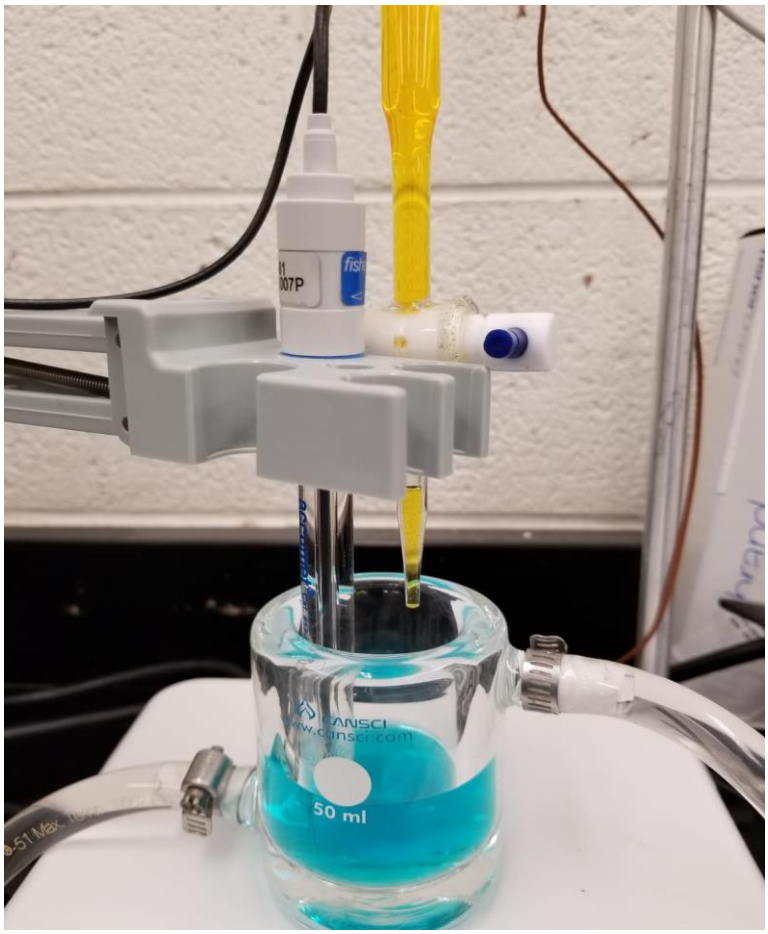


***Illustration 4 - 2 A 50 ml jacketed beaker with 25 ml of analyte (Cu liquor), a pH/ORP combination electrode and 50 ml volumetric burette with titrant (cerium sulfate).***

Illustration 4-3 shows the complete setup for titration; an accumet AB200 was used to observed the potential of solution before titrant addition and during titrant addition in search for the end and equivalence points; temperature in the analyte was increased by a circulating bath from PolyScience and kept at constant temperature with a ±1°C accuracy. A magnetic stirrer is used in order to achieve a fast, homogeneous mixed solution at each titrant addition, and in that way obtain accurate readings from the accumet AB200.

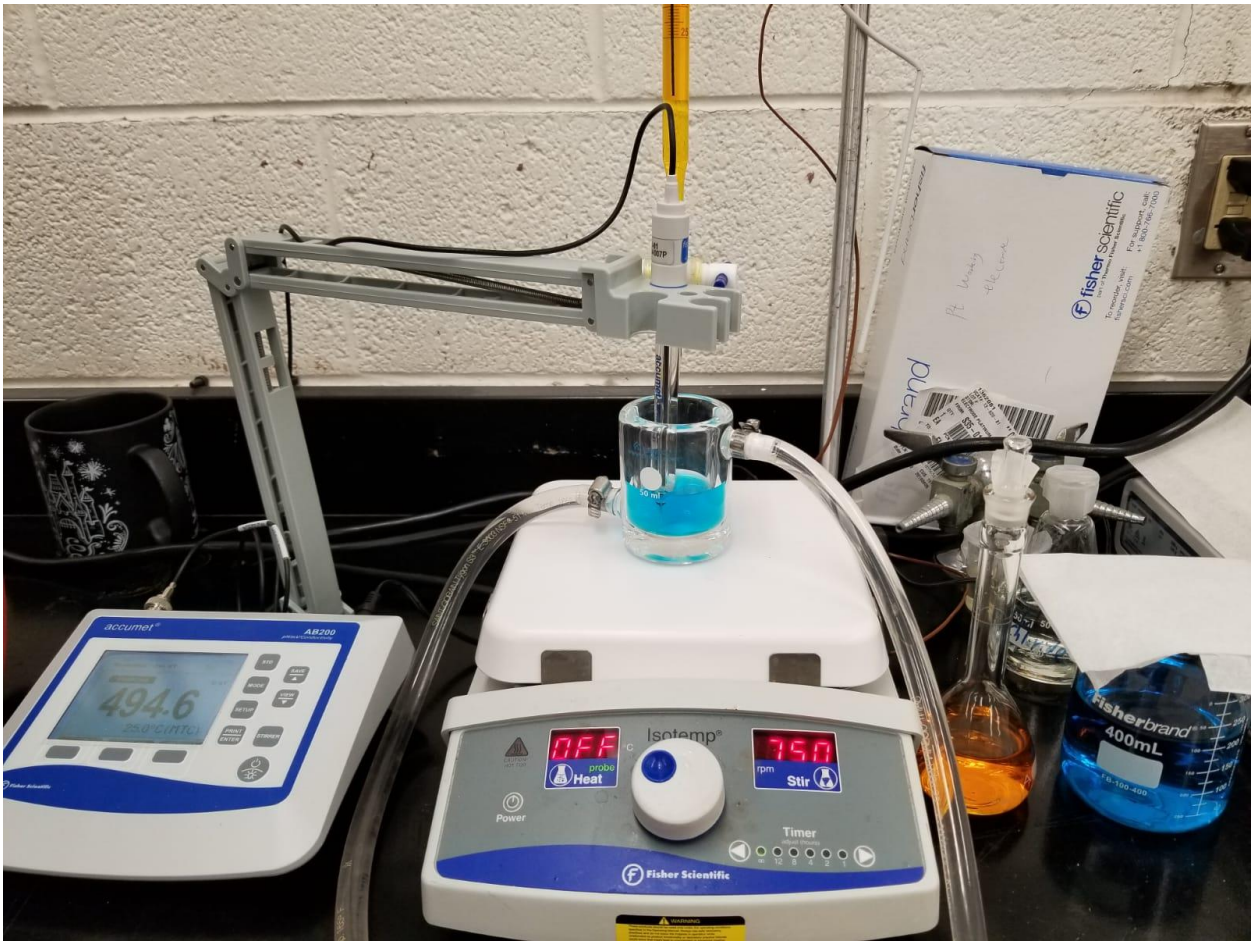


***Illustration 4 - 3*** **Complete set up of the potentiometric titration of $Fe^{2+}$ with $Ce^{4+}$**

# 5 Validation of Equation to Predict the Redox Potential of the $Fe^{3+}/Fe^{2+}$ Couple from 25℃ to 70℃

## 5.1 Introduction

As discussed in the introduction, the work in the present chapter was initiated to validate a mathematical relationship of the quaternary $H_2SO_4$-$Fe_2(SO_4)_3$-$FeSO_4$-$H_2O$ developed by Yue et al. [2]. According to Yue et al. [9, 22, 23] the redox potential of the $H_2SO_4$-$Fe_2(SO_4)_3$-$FeSO_4$-$H_2O$ system can be predicted by the following expression based on Nernst equation:

$$E(mV) = -1 \times 10^{-3} \times [T(K)]^2 + 0.91 \times T(K) + \frac{2.303R}{nF} \times T(K) \times 10^3 \times log \frac{C_{ferric,nominal}}{C_{ferrous,nominal}} + 492 \qquad (2.7)$$

where it can be observed that the overall potential of the cell can be determined by the nominal ferric/ferrous ratio and temperature. In this work, cupric ions will be added to a selected-ferric/ferrous ratio electrolytes to evaluate the effects of their present in the measured and calculated redox potentials. Measured values in this work were compared to those predicted by the above equation in order to assess its applicability.

## 5.2 Results and Discussion

The following data presents a comparison of the redox potential between experimental measurements and calculated values in synthetic electrolytes. Table 5-1 shows synthetic solutions imitating those employed in the electrorefining of copper [1, 31, 46] with a total iron concentration of 3 g/L, nominal $Fe^{3+}/Fe^{2+}$ ratios of 10:1, 2:1, 1:1, 1:2, 1:10 and 170 g/L of $H_2SO_4$ for the following temperatures: 25, 35, 45, 55, 60, 65 and 70°C.

Nominal ferric/ferrous ratios are inversely varied to observe the potential change more clearly and also observe equation's accuracy in detail. As shown in Figure 5-1, the measured potentials (corrected vs SHE at 25°C) are in well agreement with calculated potentials over a wide range of chemical compositions and temperatures from 25 to 70°C. The ORP measured showed differences of no more than 3 mV when compared to calculated values. These results validate the accuracy of the equation to predict the redox potential of the system and is applicability over a wide range of chemical compositions and over a wide range of temperatures.

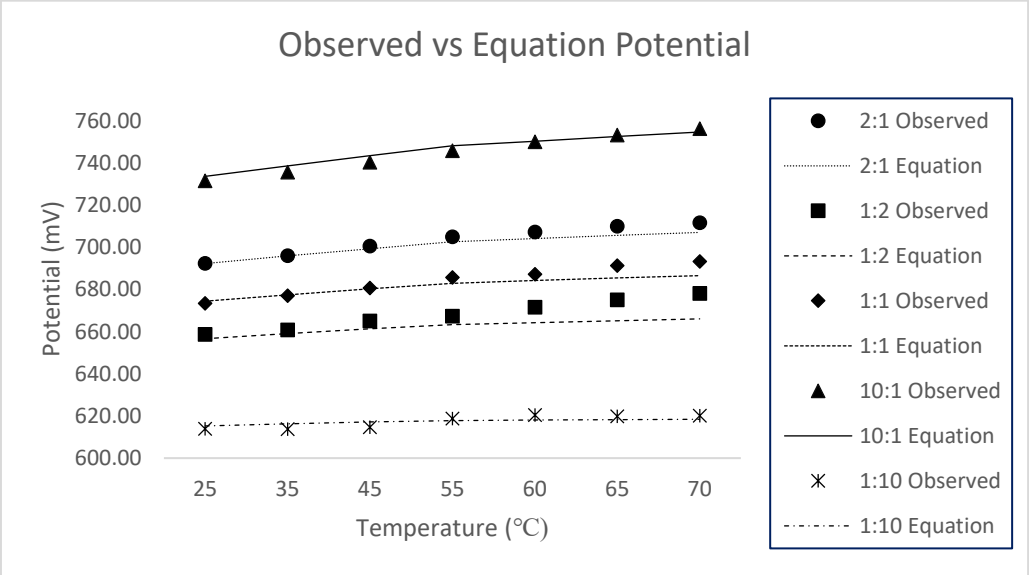


***Figure 5-1 Comparison of measured redox potentials vs calculated potentials from equation (2.7).***

***Table 5-1 Results of synthetic solutions simulating copper electrorefining electrolytes at temperatures from 25 to 70°C under 5 different nominal $Fe^{3+}/Fe^{2+}$ ratios.***

| Chemical Analysis | | Experimental results measured in the lab | | | | | | | Calculated redox potential by Equation | | Corrected $E_b$ |
|---|---|---|---|---|---|---|---|---|---|---|---|
| Test | Assay | $Fe_{total}$ g/L | $Fe^{3+}$ g/L | $Fe^{2+}$ g/L | $Cu^{2+}$ g/L | $H_2SO_4$ g/L | T °C | $E_b$ (obs) mV | $Fe^{3+}/Fe^{2+}$ Nominal | E (Calc) mV | E (Meas) mV |
| 1 | 1 | 3 | 2 | 1 | 0 | 170 | 25 | 495.33 | 2:1 | 692.33 | 692.234 |
| | 2 | 3 | 2 | 1 | 0 | 170 | 35 | 506.68 | 2:1 | 695.95 | 695.868 |
| | 3 | 3 | 2 | 1 | 0 | 170 | 45 | 519.25 | 2:1 | 700.52 | 699.303 |
| | 4 | 3 | 2 | 1 | 0 | 170 | 55 | 531.83 | 2:1 | 704.88 | 702.537 |
| | 5 | 3 | 2 | 1 | 0 | 170 | 60 | 538.27 | 2:1 | 707.10 | 704.079 |
| | 6 | 3 | 2 | 1 | 0 | 170 | 65 | 545.32 | 2:1 | 709.93 | 705.572 |
| | 7 | 3 | 2 | 1 | 0 | 170 | 70 | 551.15 | 2:1 | 711.52 | 707.014 |
| 2 | 8 | 3 | 1 | 2 | 0 | 170 | 25 | 461.29 | 1:2 | 658.28 | 656.612 |
| | 9 | 3 | 1 | 2 | 0 | 170 | 35 | 473.25 | 1:2 | 662.52 | 659.052 |
| | 10 | 3 | 1 | 2 | 0 | 170 | 45 | 483.68 | 1:2 | 664.94 | 661.291 |
| | 11 | 3 | 1 | 2 | 0 | 170 | 55 | 490.12 | 1:2 | 663.17 | 663.331 |
| | 12 | 3 | 1 | 2 | 0 | 170 | 60 | 495.33 | 1:2 | 664.17 | 664.276 |
| | 13 | 3 | 1 | 2 | 0 | 170 | 65 | 501.46 | 1:2 | 666.07 | 665.171 |
| | 14 | 3 | 1 | 2 | 0 | 170 | 70 | 508.21 | 1:2 | 668.58 | 666.015 |
| 3 | 15 | 3 | 1.5 | 1.5 | 0 | 170 | 25 | 476.30 | 1:1 | 673.29 | 674.423 |
| | 16 | 3 | 1.5 | 1.5 | 0 | 170 | 35 | 487.74 | 1:1 | 677.01 | 677.460 |
| | 17 | 3 | 1.5 | 1.5 | 0 | 170 | 45 | 499.32 | 1:1 | 680.58 | 680.297 |
| | 18 | 3 | 1.5 | 1.5 | 0 | 170 | 55 | 512.51 | 1:1 | 685.56 | 682.934 |
| | 19 | 3 | 1.5 | 1.5 | 0 | 170 | 60 | 518.33 | 1:1 | 687.17 | 684.178 |
| | 20 | 3 | 1.5 | 1.5 | 0 | 170 | 65 | 526.61 | 1:1 | 691.22 | 685.371 |
| | 21 | 3 | 1.5 | 1.5 | 0 | 170 | 70 | 532.77 | 1:1 | 693.14 | 686.515 |
| 4 | 22 | 3 | 10 | 1 | 0 | 170 | 25 | 534.36 | 10:1 | 731.36 | 733.590 |
| | 23 | 3 | 10 | 1 | 0 | 170 | 35 | 546.24 | 10:1 | 735.51 | 738.611 |
| | 24 | 3 | 10 | 1 | 0 | 170 | 45 | 559.00 | 10:1 | 740.27 | 743.433 |
| | 25 | 3 | 10 | 1 | 0 | 170 | 55 | 572.68 | 10:1 | 745.73 | 748.054 |
| | 26 | 3 | 10 | 1 | 0 | 170 | 60 | 581.02 | 10:1 | 749.86 | 750.290 |
| | 27 | 3 | 10 | 1 | 0 | 170 | 65 | 588.47 | 10:1 | 753.08 | 752.476 |
| | 28 | 3 | 10 | 1 | 0 | 170 | 70 | 595.72 | 10:1 | 756.09 | 754.612 |
| 5 | 29 | 3 | 1 | 10 | 0 | 170 | 25 | 416.81 | 1:10 | 613.81 | 615.256 |
| | 30 | 3 | 1 | 10 | 0 | 170 | 35 | 424.48 | 1:10 | 613.75 | 616.309 |
| | 31 | 3 | 1 | 10 | 0 | 170 | 45 | 433.38 | 1:10 | 614.64 | 617.161 |
| | 32 | 3 | 1 | 10 | 0 | 170 | 55 | 445.64 | 1:10 | 618.70 | 617.814 |
| | 33 | 3 | 1 | 10 | 0 | 170 | 60 | 451.47 | 1:10 | 620.31 | 618.065 |
| | 34 | 3 | 1 | 10 | 0 | 170 | 65 | 455.15 | 1:10 | 619.76 | 618.266 |
| | 35 | 3 | 1 | 10 | 0 | 170 | 70 | 459.75 | 1:10 | 620.12 | 618.418 |

It can be noticed from figure 5-1 a more pronounced difference between potentials as temperature increase and a difference of more than 3 mV is reached at 65 and 70°C in ratios of 2:1 and 1:1. This is attributed to a decompensation in temperature of the circulating bath when reaches high temperatures (55 to 70°C); it seems that while working on getting a new higher temperature, the work done overpasses the desired temperature and then decrease it back to set value.

The applicability of the equation is also investigated in synthetic solutions typically employed in copper electrowinning [1, 42, 43, 48]. With the purpose to expand the scope of the equation, total Fe concentrations were set to 6 g/L in these set of experiments, nominal $Fe^{3+}/Fe^{2+}$ ratios of 100:1, 5:1, 1:5 and 1:100; 200 g/L of $H_2SO_4$ and temperatures from 25 to 70°C as shown in table 5-2.

This confirms the applicability and veracity of the equation under expanded chemical concentrations. From these results we can conclude that redox potentials can and are well predicted by the equation based only on nominal $Fe^{3+}/Fe^{2+}$ ratio and temperature. It was also shown that acid concentration in both extremes of the most used copper liquors (170-200 g/L) under both processes (electrorefining and electrowinning) has no significant effect in the overall potential. The difference between the calculated and measured potentials was under 3 mV, where an isolated difference of 3.6 mV is observed in the 1:5 ratio at 70°C, attributed to a temperature compensation of the circulating bath.

***Table 5-2 Results of synthetic solutions simulating copper electrowinning electrolytes at temperatures from 25 to 70°C under 4 different nominal $Fe^{3+}/Fe^{2+}$ ratios.***

| Chemical Analysis | | Experimental results measured in the lab | | | | | | | Calculated redox potential by Equation | | Corrected $E_b$ |
|---|---|---|---|---|---|---|---|---|---|---|---|
| Test | Assay | $Fe_{total}$ g/L | $Fe^{3+}$ g/L | $Fe^{2+}$ g/L | $Cu^{2+}$ g/L | $H_2SO_4$ g/L | T °C | $E_b$ (obs) mV | $Fe^{3+}/Fe^{2+}$ Nominal | E (Calc) mV | E (Meas) mV |
| 6 | 36 | 6 | 5 | 1 | 0 | 200 | 25 | 516.186 | 2:1 | 715.779 | 713.182 |
| | 37 | 6 | 5 | 1 | 0 | 200 | 35 | 528.454 | 2:1 | 720.203 | 717.725 |
| | 38 | 6 | 5 | 1 | 0 | 200 | 45 | 541.95 | 2:1 | 724.427 | 723.215 |
| | 39 | 6 | 5 | 1 | 0 | 200 | 55 | 555.445 | 2:1 | 728.451 | 728.498 |
| | 40 | 6 | 5 | 1 | 0 | 200 | 60 | 562.806 | 2:1 | 730.388 | 731.642 |
| | 41 | 6 | 5 | 1 | 0 | 200 | 65 | 569.553 | 2:1 | 732.275 | 734.161 |
| | 42 | 6 | 5 | 1 | 0 | 200 | 70 | 575.995 | 2:1 | 734.112 | 736.362 |
| 7 | 43 | 6 | 5.94 | .0594 | 0 | 200 | 25 | 594.396 | 100:1 | 791.392 | 792.757 |
| | 44 | 6 | 5.94 | .0594 | 0 | 200 | 35 | 608.505 | 100:1 | 797.776 | 799.763 |
| | 45 | 6 | 5.94 | .0594 | 0 | 200 | 45 | 624.76 | 100:1 | 806.025 | 806.569 |
| | 46 | 6 | 5.94 | .0594 | 0 | 200 | 55 | 641.629 | 100:1 | 814.682 | 813.175 |
| | 47 | 6 | 5.94 | .0594 | 0 | 200 | 60 | 646.843 | 100:1 | 815.679 | 816.403 |
| | 48 | 6 | 5.94 | .0594 | 0 | 200 | 65 | 655.124 | 100:1 | 819.732 | 819.581 |
| | 49 | 6 | 5.94 | .0594 | 0 | 200 | 70 | 662.872 | 100:1 | 823.239 | 822.709 |
| 8 | 50 | 6 | .0594 | 5.94 | 0 | 200 | 25 | 360.023 | 1:100 | 557.019 | 556.089 |
| | 51 | 6 | .0594 | 5.94 | 0 | 200 | 35 | 365.593 | 1:100 | 554.864 | 555.157 |
| | 52 | 6 | .0594 | 5.94 | 0 | 200 | 45 | 372.341 | 1:100 | 553.606 | 554.025 |
| | 53 | 6 | .0594 | 5.94 | 0 | 200 | 55 | 381.235 | 1:100 | 554.288 | 552.693 |
| | 54 | 6 | .0594 | 5.94 | 0 | 200 | 60 | 383.689 | 1:100 | 552.525 | 551.953 |
| | 55 | 6 | .0594 | 5.94 | 0 | 200 | 65 | 386.756 | 1:100 | 551.364 | 551.162 |
| | 56 | 6 | .0594 | 5.94 | 0 | 200 | 70 | 390.437 | 1:100 | 550.804 | 550.320 |
| 9 | 57 | 6 | 1 | 5 | 0 | 200 | 25 | 436.136 | 1:5 | 633.132 | 633.067 |
| | 58 | 6 | 1 | 5 | 0 | 200 | 35 | 443.497 | 1:5 | 632.768 | 634.717 |
| | 59 | 6 | 1 | 5 | 0 | 200 | 45 | 454.945 | 1:5 | 636.210 | 636.167 |
| | 60 | 6 | 1 | 5 | 0 | 200 | 55 | 465.886 | 1:5 | 638.939 | 637.417 |
| | 61 | 6 | 1 | 5 | 0 | 200 | 60 | 470.794 | 1:5 | 639.630 | 637.967 |
| | 62 | 6 | 1 | 5 | 0 | 200 | 65 | 476.621 | 1:5 | 641.229 | 638.467 |
| | 63 | 6 | 1 | 5 | 0 | 200 | 70 | 482.142 | 1:5 | 642.509 | 638.917 |

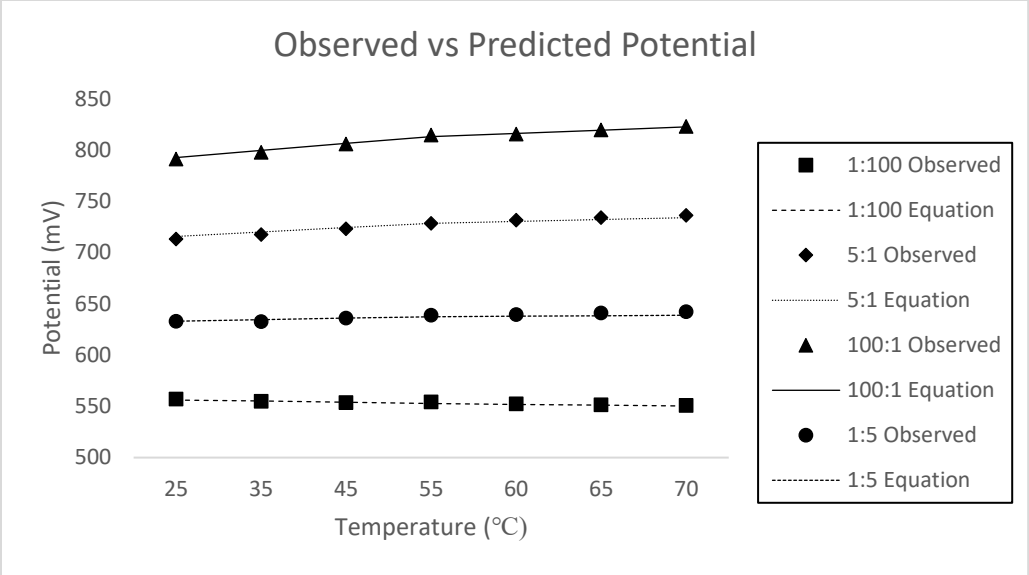


***Figure 5-2 Comparison of the measured redox potentials vs calculated potentials from equation (2.7).***

As can be seen in figure 5-2, higher potentials are seen under higher nominal $Fe^{3+}/Fe^{2+}$ ratios, where the highest potential is under the 100:1 nominal $Fe^{3+}/Fe^{2+}$ ratio, and the lowest potential under its reciprocal, 1:100.

Finally, Copper is added to a selected group of nominal $Fe^{3+}/Fe^{2+}$ ratio to cover both copper electrometallurgical processes, winning and refining, in order to further test the applicability of the equation. It was found that the presence of copper in the electrolyte has no effect in the redox potential of the $H_2SO_4$-$CuSO_4$-$Fe_2(SO_4)_3$-$FeSO_4$-$H_2O$ system under the nominal $Fe^{3+}/Fe^{2+}$ ratios of 2:1, 5:1, 10:1 and 1:5 with copper concentrations ranging from 36 to 50 g/L, as shown in table 5-3. From the previously, it can be assumed that a similar behavior (no significant influence of copper concentration in the overall potential of the cell) can be expected at any nominal ratio and similar copper concentrations (employed in industry).

***Table 5-3 Results of synthetic solutions simulating copper electrolytes at temperatures from 25 to 70°C. Different copper concentrations were added to 7 different chemical compositions of selected nominal $Fe^{3+}/Fe$ ratios.***

| Chemical Analysis | | Experimental results measured in the lab | | | | | | | Calculated redox potential by Equation | | Corrected $E_b$ |
|---|---|---|---|---|---|---|---|---|---|---|---|
| Test | Assay | $Fe_{total}$ g/L | $Fe^{3+}$ g/L | $Fe^{2+}$ g/L | $Cu^{2+}$ g/L | $H_2SO_4$ g/L | T °C | $E_b$ (obs) mV | $Fe^{3+}/Fe^{2+}$ Nominal | E (Calc) mV | E (Meas) mV |
| 10 | 64 | 6 | 4 | 2 | 36 | 200 | 25 | 495.944 | 2:1 | 692.940 | 692.234 |
| | 65 | 6 | 4 | 2 | 36 | 200 | 35 | 506.372 | 2:1 | 695.643 | 695.869 |
| | 66 | 6 | 4 | 2 | 36 | 200 | 45 | 518.026 | 2:1 | 699.291 | 699.303 |
| | 67 | 6 | 4 | 2 | 36 | 200 | 55 | 531.215 | 2:1 | 704.268 | 702.537 |
| | 68 | 6 | 4 | 2 | 36 | 200 | 60 | 535.202 | 2:1 | 704.038 | 704.079 |
| | 69 | 6 | 4 | 2 | 36 | 200 | 65 | 541.643 | 2:1 | 706.251 | 705.572 |
| | 70 | 6 | 4 | 2 | 36 | 200 | 70 | 548.39 | 2:1 | 708.757 | 707.014 |
| 11 | 71 | 2.4 | 2 | 0.4 | 36 | 200 | 25 | 519.56 | 5:1 | 716.556 | 715.779 |
| | 72 | 2.4 | 2 | 0.4 | 36 | 200 | 35 | 530.908 | 5:1 | 720.179 | 720.203 |
| | 73 | 2.4 | 2 | 0.4 | 36 | 200 | 45 | 543.176 | 5:1 | 724.441 | 724.427 |
| | 74 | 2.4 | 2 | 0.4 | 36 | 200 | 55 | 556.068 | 5:1 | 729.121 | 728.451 |
| | 75 | 2.4 | 2 | 0.4 | 36 | 200 | 60 | 561.272 | 5:1 | 730.108 | 730.388 |
| | 76 | 2.4 | 2 | 0.4 | 36 | 200 | 65 | 567.713 | 5:1 | 732.321 | 732.275 |
| | 77 | 2.4 | 2 | 0.4 | 36 | 200 | 70 | 575.381 | 5:1 | 735.748 | 734.112 |
| 12 | 78 | 2.2 | 2 | 0.2 | 40 | 200 | 25 | 533.668 | 10:1 | 730.664 | 733.59 |
| | 79 | 2.2 | 2 | 0.2 | 40 | 200 | 35 | 545.63 | 10:1 | 734.901 | 738.612 |
| | 80 | 2.2 | 2 | 0.2 | 40 | 200 | 45 | 559.86 | 10:1 | 741.125 | 743.433 |
| | 81 | 2.2 | 2 | 0.2 | 40 | 200 | 55 | 572.313 | 10:1 | 745.366 | 748.054 |
| | 82 | 2.2 | 2 | 0.2 | 40 | 200 | 60 | 579.981 | 10:1 | 748.817 | 750.290 |
| | 83 | 2.2 | 2 | 0.2 | 40 | 200 | 65 | 585.809 | 10:1 | 750.417 | 752.476 |
| | 84 | 2.2 | 2 | 0.2 | 40 | 200 | 70 | 592.863 | 10:1 | 753.230 | 754.612 |
| 13 | 85 | 3 | 0.5 | 2.5 | 40 | 200 | 25 | 438.9 | 1:5 | 635.896 | 633.067 |
| | 86 | 3 | 0.5 | 2.5 | 40 | 200 | 35 | 448.4 | 1:5 | 637.671 | 634.717 |
| | 87 | 3 | 0.5 | 2.5 | 40 | 200 | 45 | 455.765 | 1:5 | 637.030 | 636.167 |
| | 88 | 3 | 0.5 | 2.5 | 40 | 200 | 55 | 465.886 | 1:5 | 638.939 | 637.417 |
| | 89 | 3 | 0.5 | 2.5 | 40 | 200 | 60 | 470.18 | 1:5 | 639.016 | 637.967 |
| | 90 | 3 | 0.5 | 2.5 | 40 | 200 | 65 | 476.928 | 1:5 | 641.536 | 638.467 |
| | 91 | 3 | 0.5 | 2.5 | 40 | 200 | 70 | 481.835 | 1:5 | 642.202 | 638.917 |
| 14 | 92 | 6 | 5.459 | 0.545 | 45 | 200 | 25 | 536.736 | 10:1 | 733.732 | 733.632 |
| | 93 | 6 | 5.459 | 0.545 | 45 | 200 | 35 | 545.323 | 10:1 | 734.594 | 738.655 |
| | 94 | 6 | 5.459 | 0.545 | 45 | 200 | 45 | 560.659 | 10:1 | 741.924 | 743.478 |
| | 95 | 6 | 5.459 | 0.545 | 45 | 200 | 55 | 574.154 | 10:1 | 747.207 | 748.101 |
| | 96 | 6 | 5.459 | 0.545 | 45 | 200 | 60 | 579.981 | 10:1 | 748.817 | 750.338 |
| | 97 | 6 | 5.459 | 0.545 | 45 | 200 | 65 | 586.115 | 10:1 | 750.723 | 752.524 |
| | 98 | 6 | 5.459 | 0.545 | 45 | 200 | 70 | 593.476 | 10:1 | 753.843 | 754.660 |
| 15 | 99 | 3 | 2 | 1 | 45 | 200 | 25 | 495.33 | 2:1 | 692.326 | 692.234 |
| | 100 | 3 | 2 | 1 | 45 | 200 | 35 | 503.918 | 2:1 | 693.189 | 695.869 |
| | 101 | 3 | 2 | 1 | 45 | 200 | 45 | 515.573 | 2:1 | 696.838 | 699.303 |
| | 102 | 3 | 2 | 1 | 45 | 200 | 55 | 528.148 | 2:1 | 701.201 | 702.537 |
| | 103 | 3 | 2 | 1 | 45 | 200 | 60 | 534.282 | 2:1 | 703.118 | 704.079 |
| | 104 | 3 | 2 | 1 | 45 | 200 | 65 | 540.416 | 2:1 | 705.024 | 705.572 |
| | 105 | 3 | 2 | 1 | 45 | 200 | 70 | 547.164 | 2:1 | 707.531 | 707.014 |
| 16 | 106 | 3 | 2 | 1 | 50 | 200 | 25 | 497.17 | 2:1 | 694.166 | 692.234 |
| | 107 | 3 | 2 | 1 | 50 | 200 | 35 | 506.065 | 2:1 | 695.336 | 695.869 |
| | 108 | 3 | 2 | 1 | 50 | 200 | 45 | 517.72 | 2:1 | 698.985 | 699.303 |
| | 109 | 3 | 2 | 1 | 50 | 200 | 55 | 530.295 | 2:1 | 703.348 | 702.537 |
| | 110 | 3 | 2 | 1 | 50 | 200 | 60 | 535.202 | 2:1 | 704.038 | 704.079 |
| | 111 | 3 | 2 | 1 | 50 | 200 | 65 | 541.95 | 2:1 | 706.558 | 705.572 |
| | 112 | 3 | 2 | 1 | 50 | 200 | 70 | 548.084 | 2:1 | 708.451 | 707.014 |

From figure 5-3, we can observe that the measured redox potentials are in good agreement with those calculated redox potentials, over a wide range of solution compositions. It can be noticed how measured redox potentials of equal nominal $Fe^{3+}/Fe^{2+}$ ratios overlap, in well agreement with calculated potentials from equation. These ratios (10:1 and 2:1) overlap although their copper concentration differ, 40 and 45 g/L in the 10:1 nominal ratio, and 36, 45 and 50 g/L of copper in the 2:1, confirming that the overall redox potential of the cell is solely determined by temperature and nominal $Fe^{3+}/Fe^{2+}$ ratio. This further confirms the wide applicability of the equation (Eq. (1)) in acidic iron sulfate solutions a wide range of copper concentrations, from 36 to 50 g/L, proving the little or almost none effect of Cu ions in the overall potential of the cell.

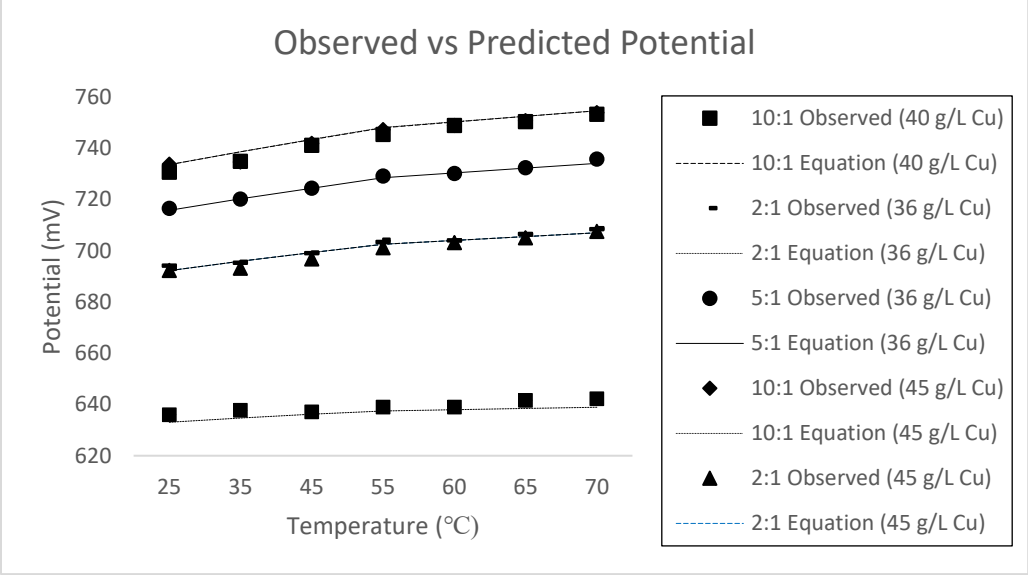


***Figure 5-3 Comparison of the measured redox potentials vs calculated potentials from equation (2.7).***

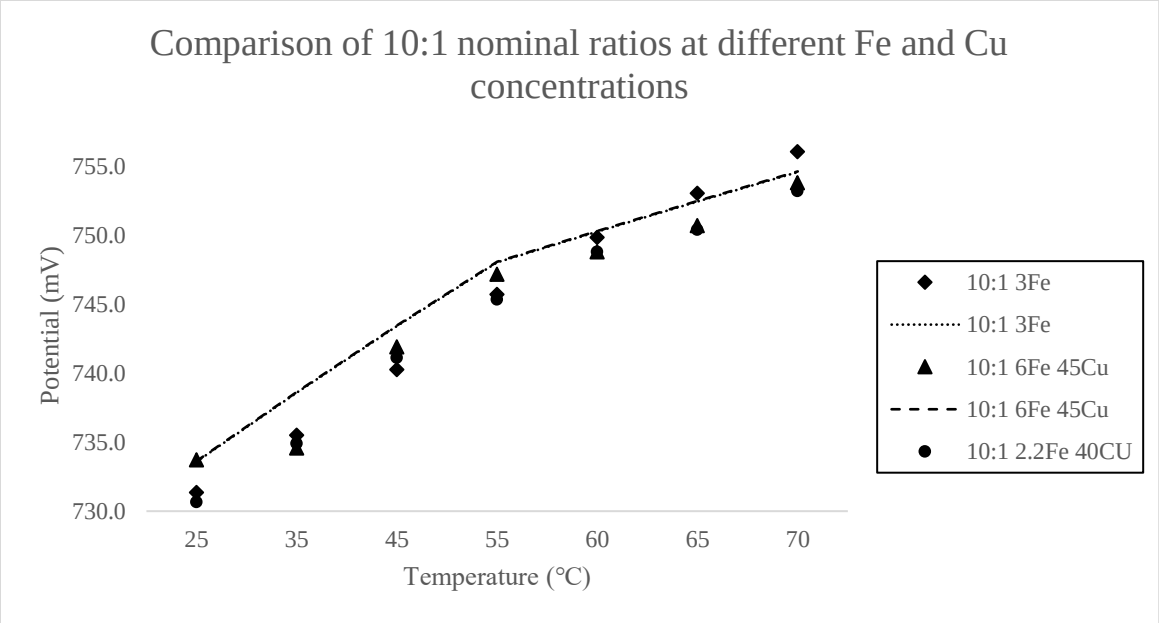


***Figure 5-4 Comparison of the measured redox potentials of different chemical composition solutions vs calculated potentials from Eq. (2.7) under the same nominal $Fe^{3+}/Fe^{2+}$ ratio under temperatures from 25 to 70°C.***

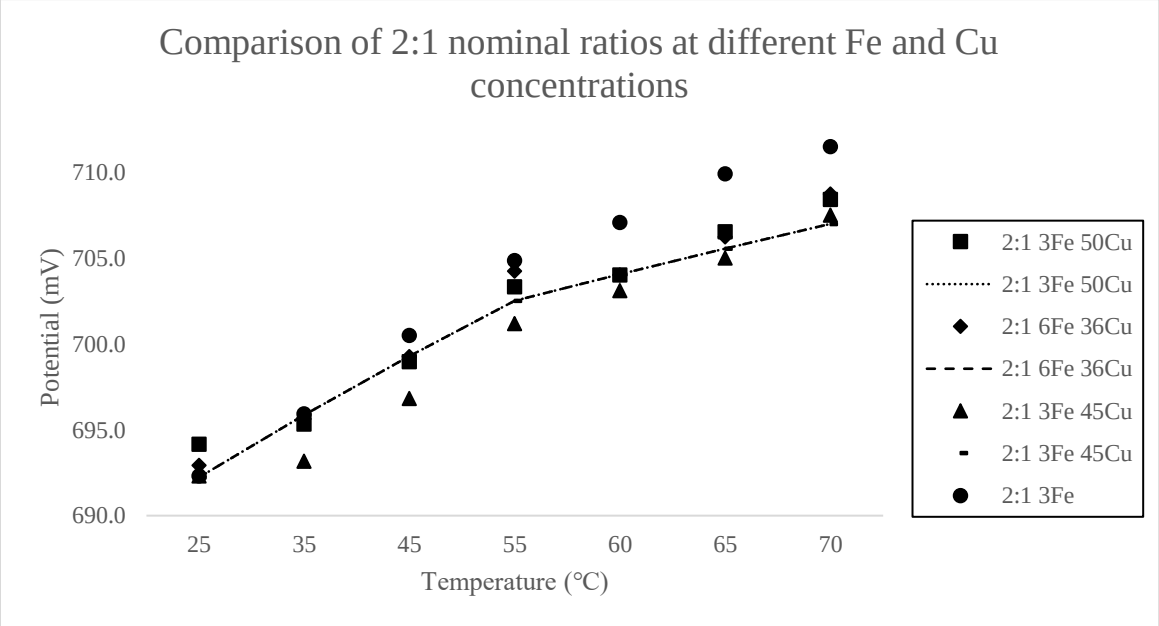


***Figure 5-5 Comparison of the measured redox potentials of solutions with different chemical composition vs calculated potentials from Eq. (2.7) under the same nominal $Fe^{3+}/Fe^{2+}$ ratio under temperatures from 25 to 70°C.***

## 5.3 Summary

The potentials calculated shown in table 5-1, 5-2 and 5-3 under a nominal $Fe^{3+}/Fe^{2+}$ ratio of 2:1 are compared in figure 5-4. Four different solutions with the following compositions are studied: 1) 3 g/L Fe, 170 g/L $H_2SO_4$; 2) 3 g/L Fe, 45 g/L Cu, 200 g/L $H_2SO_4$; 3) 3 g/L Fe, 50 g/L Cu, 200 g/L $H_2SO_4$; and 4) 6 g/L Fe, 36 g/L Cu, 200 g/L $H_2SO_4$. As we can see, all four potentials agree very well with each other following the predicted potential, with differences under 3 mV, with the exception of solution 1, with a difference from calculated potential of 4.4 and 4.5 mV at 65 and 70°C, respectively.

In the same manner, calculated potentials shown in table 5-1, 5-2 and 5-3 under a nominal $Fe^{3+}/Fe^{2+}$ ratio of 10:1 are compared in figure 5-5. Three different solutions with the following compositions are studied: 1) 3 g/L Fe, 170 g/L $H_2SO_4$; 2) 6 g/L Fe, 45 g/L Cu, 200 g/L $H_2SO_4$; and 3) 2.2 g/L Fe, 40 g/L Cu, 200 g/L $H_2SO_4$. Compared potentials are in well agreement with each other and with calculated potential from equation, within 3 mV difference among themselves and/or calculated potential. In both figures, 5-4 and 5-5 it is demonstrated that under each nominal ferric/ferrous ratio, the measured redox potentials is then solely dependent on the variable of temperature.

It is demonstrated that for each nominal ferric/ferrous ratio, the measured redox potential can be solely determined by nominal ferric to ferrous ratio. The measured redox potentials at a temperature of 25°C were compared to results from literature [42, 43, 44] and further support the validity of equation (2.7) and the results done in this work in acidic iron sulfate solution containing cupric ions.

These findings support that Eq. 2.7 developed by Yue et al. can be employed to predict the redox potential of the aqueous $H_2SO_4$-$Fe_2(SO_4)_3$-$FeSO_4$-$H_2O$ and $H_2SO_4$-$CuSO_4$-$Fe_2(SO_4)_3$-$FeSO_4$-$H_2O$ system and further expand its applicability to broader nominal ferric/ferrous ratios and higher acid concentrations. It also help to understand electrochemical kinetics of iron under such conditions based on the measured redox potential during Cu electrowinning and electrorefining.

The applicability of Eq. (2.7) in the aqueous $H_2SO_4$-$Fe_2(SO_4)_3$-$FeSO_4$-$H_2O$ solution is validated over a wide range of temperatures and Cu concentrations. It was also observed that Cu ions up to 50 g/L exerted no significant effect on the prediction accuracy of the Eq. (2.7) model.

# 6 Determination of Iron (II) in the $H_2SO_4$-$Fe_2(SO_4)_3$-$FeSO_4$-$H_2O$ and the $H_2SO_4$-$CuSO_4$-$Fe_2(SO_4)_3$-$FeSO_4$-$H_2O$ Systems from 25℃ to 70℃

## 6.1 Introduction

The work in this chapter is aimed to further determine the real concentrations of ferrous ions in the quaternary $H_2SO_4$-$Fe_2(SO_4)_3$-$FeSO_4$-$H_2O$ system in terms of temperature. 125 ml of the prepared electrolytes mentioned in previous chapter were taken a side of the ORP test and subjected to a potentiometric titration with Cerium(IV) following the 1 to 1. $Ce^{4+}$ reacts with $Fe^{2+}$ according to the following reaction:

$$Ce^{4+} + Fe^{2+} \rightleftharpoons Ce^{3+} + Fe^{3+} \tag{6.1}$$

Separated into 2 half reactions and measure each standard potential, which are the dependent variables of the concentration of the titrant:

$$Ce^{4+} + e^- \rightleftharpoons Ce^{3+} \qquad \text{(reduction of } Ce^4\text{, } E^0 = 1.70 \text{ V)} \tag{6.2}$$

$$Fe^{2+} \rightleftharpoons Fe^{3+} + e^- \qquad \text{(oxidation of } Fe^2\text{, } E^0 = 0.77 \text{ V)} \tag{6.3}$$

Cerium (IV) is the oxidizing agent and iron (II) is the reducing agent, and the electrode potentials of the two half-reactions are always equal. From the two we get an equivalence point of 1.06 V according to the following stoichiometry:

$$E_{eq} = E^0_{Ce^{4+}/Ce^{3+}} - \frac{0.059}{1}\log\frac{Ce^{3+}}{Ce^{4+}} \tag{6.4}$$

$$E_{eq} = E^0_{Fe^{3+}/Fe^{2+}} - \frac{0.059}{1}\log\frac{Fe^{2+}}{Fe^{3+}} \tag{6.5}$$

$$E_{eq} = \frac{E^0_{Fe^{3+}/Fe^{2+}} + E^0_{Ce^{4+}/Ce^{3+}}}{2} \tag{6.6}$$

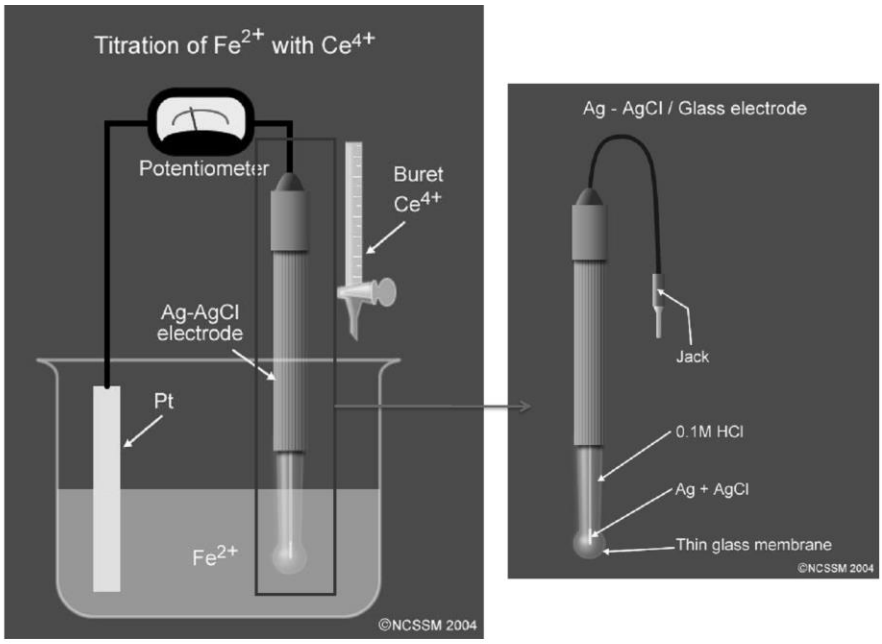


***Illustration 6 - 1 Schematic of the redox titration of $Fe^{2+}$ with $Ce^{4+}$, North Carolina School of Science and Mathematics.***

The system's potential ($E_{system}$) for an oxidation/reduction titration is usually independent of dilution. Consequently, titration curves for oxidation/reduction reactions are usually independent of analyte and reagent concentrations, in contrast with other types of titration curves [4, 38, 39]. The completion of the reaction is described by the equilibrium constant ($K_{eq}$), the change in potential in the equivalence-point region of an oxidation/reduction titration becomes larger as the reaction becomes more complete, like a larger $K_{eq}$. The greater the difference in reduction potential, the larger the reaction potential, the more reaction complete. Air oxidation of iron(II) takes place rapidly in neutral solutions but is inhibited in the presence of acids, with the most stable preparations being about 0.5 M in $H_2SO_4$ and no more than one day. Both cerium (IV) and permanganate are strong oxidizing agents. Solutions of Ce(IV) in sulfuric acid are stable indefinitely, whereas permanganate is not. A further advantage of cerium is that a primary-standard

grade salt of the reagent is available, thus making possible the direct preparation of standard solutions. Despite these advantages of cerium solutions over permanganate solutions the latter are more widely used. One reason is the color of permanganate solutions, which is intense enough to serve as an indicator in titrations. A second reason for the popularity of permanganate solutions is their modest cost.

With each addition of ceric sulfate, the above redox reaction (Eq. 6.1) occurs, oxidizing $Fe^{2+}$ to $Fe^{3+}$ and changing the potential of the electrolyte (increasing it). This potential is monitored by the indicator electrode (Pt Ag/AgCl combination electrode) and meter (Accumet AB200) until the equivalence point is reached, where the titrant amount added (ml) is recorded. Titrant is continuously added until the endpoint is reached, and a titration curve can be drawn. Measured values in this work were compared to the initial intended amount of Fe (II) added to check the error percentage.

## 6.2 Results and Discussion

The following data shows the results of the redox potentiometric determination of ferrous iron with ceric sulfate against the acidic iron sulfate solution. The measurements of the ferrous iron concentration where compared vs the initial values in synthetic electrolytes at each temperature. Table 6.1 shows this comparison in $H_2SO_4$-$Fe_2(SO_4)_3$-$FeSO_4$-$H_2O$ and $CuSO_4$-$H_2SO_4$-$Fe_2(SO_4)_3$-$FeSO_4$-$H_2O$ systems, with total iron concentrations from 2.2 to 6 g/L (0.04 to 0.11 mol/L), nominal $Fe^{3+}/Fe^{2+}$ ratios of 100:1, 10:1, 5:1, 2:1, 1:1, 1:2, 1:5, 1:10, 1:100 and acid concentrations of 170 and 200 g/L (1.7 to 2M) of $H_2SO_4$ for the following temperatures: 25, 35, 45, 55, 60, 65 and 70°C. The inversely varied ferric/ferrous ratios allowed for a marked observation of the sensitivity and accuracy of the method. As shown in table 6.1, the initial ferrous iron concentrations (corrected vs SHE at 25°C) are in well agreement with those measured under potentiometric determination over a wide range of chemical compositions and temperatures from 25 to 70°C.

The measured $Fe^{2+}$ concentration showed an average difference of 2.53 % when compared to initial values. These results indicate an acceptable accuracy of the initial values of ferrous iron in both $H_2SO_4$-$Fe_2(SO_4)_3$-$FeSO_4$-$H_2O$ and $CuSO_4$-$H_2SO_4$-$Fe_2(SO_4)_3$-$FeSO_4$-$H_2O$ systems and is therefore a sizable validation of the ORP test. It can be noticed however, higher averages of 3.8 and 3.5 percent in terms of temperature, 35 and 60°C, respectively. Similarly, averages of 3.9 and 3.4 percent were obtained at nominal ratios of 1:1 and 2:1, respectively. Nevertheless, no real pattern was observed in terms of temperature or nominal ratios.

Figure 6-2 shows the logarithmic relationship between electrode potential and concentration cerium(IV), the analyte. The electrode potentials for the two half-reactions are always identical at the equivalence point, where theoretically the concentration of cerium(IV) and iron(II) are equal, according to the following equations:

$$E_{eq} = E^0_{Ce^{4+}/Ce^{3+}} - \frac{0.0592}{1} log \frac{[Ce^{3+}]}{[Ce^{4+}]} \quad (6.3)$$

$$E_{eq} = E^0_{Fe^{3+}/Fe^{2+}} - \frac{0.0592}{1} log \frac{[Fe^{2+}]}{[Fe^{3+}]} \quad (6.4)$$

$$E_{eq} = \frac{E^0_{Fe^{3+}/Fe^{2+}} + E^0_{Ce^{4+}/Ce^{3+}}}{2} \quad (6.5)$$

This relationship allowed for a relatively easy volumetric determination, a simple, accurate method analysis and helped to minimize the error of volume and indication readings, both equivalence and endpoint values. Detailed data results can be found in tables 6-2, 6-3 and 6-4 as well as in tables A-1, A-2 and A-3 in the appendix.

***Table 6-1 Calculated concentrations of $Fe^{2+}$ (mol/L) by potentiometric titration vs initial measured concentrations (mol/L) in aqueous $H_2SO_4$-$Fe_2(SO_4)_3$-$FeSO_4$-$H_2O$ and $CuSO_4$-$H_2SO_4$-$Fe_2(SO_4)_3$-$FeSO_4$-$H_2O$ solutions of different nominal $Fe^{3+}/Fe^{2+}$ ratios from 25°C to 70°C.***

| Nominal $Fe^{3+}/Fe^{2+}$ Ratio | 25°C | | | 35°C | | | 45°C | | | 55°C | | | 60°C | | | 65°C | | | 70°C | | |
|---|---|---|---|---|---|---|---|---|---|---|---|---|---|---|---|---|---|---|---|---|---|
| | $Fe^{2+}$ | $Ce^{4+}$ | % Error | $Fe^{2+}$ | $Ce^{4+}$ | % Error | $Fe^{2+}$ | $Ce^{4+}$ | % Error | $Fe^{2+}$ | $Ce^{4+}$ | % Error | $Fe^{2+}$ | $Ce^{4+}$ | % Error | $Fe^{2+}$ | $Ce^{4+}$ | % Error | $Fe^{2+}$ | $Ce^{4+}$ | % Error |
| 100:1 | .00107 | .00105 | 1.83 | .00107 | .00113 | 5.73 | .00107 | .00105 | 1.82 | .00107 | .00109 | 1.95 | .00107 | .00111 | 3.84 | .00107 | .00113 | 5.73 | .00107 | .00109 | 1.95 |
| 10:1 | .00986 | .00101 | 2.44 | .00986 | .00961 | 2.57 | .00986 | .0101 | 2.4 | .00986 | .00101 | 2.44 | .00986 | .00103 | 4..49 | .00986 | .00103 | 4.49 | .00986 | .00101 | 2.44 |
| 5:1 | .01809 | .01859 | 2.74 | .01809 | .01778 | 1.73 | .01809 | .01818 | 0.51 | .01809 | .01818 | 0.51 | .01809 | .01859 | 2.74 | .01809 | .01818 | 0.51 | .01809 | .01818 | 0.51 |
| 2:1 | .01809 | .01859 | 2.74 | .01809 | .01940 | 7.21 | .01809 | .01859 | 2.74 | .01809 | .01899 | 4.97 | .01809 | .01859 | 2.74 | .01809 | .01818 | 0.51 | .01809 | .01859 | 2.74 |
| 1:1 | .02713 | .02804 | 3.34 | .02713 | .02804 | 3.34 | .02713 | .02828 | 4.25 | .02713 | .02828 | 4.25 | .02713 | .02869 | 5.74 | .02713 | .02626 | 3.20 | .02713 | .02626 | 3.20 |
| 1:2 | .03618 | .03636 | 0.51 | .03618 | .03718 | 2.74 | .03618 | .03697 | 2.18 | .03618 | .03636 | 0.51 | .03618 | .03798 | 4.97 | .03618 | .03758 | 3.86 | .03618 | .03798 | 4.97 |
| 1:5 | .09044 | 0.0897 | 0.816 | .09044 | .09293 | 2.75 | .09044 | .09091 | 0.52 | .09044 | .09495 | 4.99 | .09044 | .09293 | 2.75 | .09044 | .09091 | 0.52 | .09044 | .08970 | 0.82 |
| 1:10 | .04884 | .04848 | 0.73 | .04884 | .04525 | 7.35 | .04884 | .04848 | 0.73 | .04884 | .04768 | 2.38 | .04884 | .04687 | 4.04 | .04884 | .04848 | 0.72 | .04884 | .04889 | 0.10 |
| 1:100 | .10744 | .10909 | 1.54 | .10744 | .10869 | 1.16 | .10744 | .10707 | 0.34 | .10744 | .10788 | 0.41 | .10744 | .10788 | 0.41 | .10744 | .10909 | 1.54 | .10744 | .10707 | 0.34 |

| Volume $Ce^{4+}$(mL) | $Fe^{3+}$ | $Fe^{2+}$ | $Ce^{3+}$ | $Ce^{4+}$ | E sys. (V) |
|---|---|---|---|---|---|
| 0.8 | 0.00310 | 0.02319 | | | 0.63 |
| 1.2 | 0.00458 | 0.02131 | | | 0.64 |
| 2 | 0.00741 | 0.01771 | | | 0.66 |
| 2.8 | 0.01007 | 0.01433 | | | 0.67 |
| 3.6 | 0.01259 | 0.01113 | | | 0.68 |
| 4.4 | 0.01497 | 0.00810 | | | 0.70 |
| 6 | 0.01935 | 0.00253 | | | 0.73 |
| 6.75 | 0.02126 | 0.00010 | | | 0.82 |
| 6.8 | | | | | 1.06 |
| 6.85 | | | 0.02130 | 0.00021 | 1.32 |
| 8 | | | 0.02055 | 0.00369 | 1.40 |
| 9.2 | | | 0.01983 | 0.00707 | 1.41 |
| 10 | | | 0.01938 | 0.00919 | 1.42 |
| 10.8 | | | 0.01895 | 0.01122 | 1.43 |
| 11.6 | | | 0.01853 | 0.01316 | 1.43 |
| 12.4 | | | 0.01814 | 0.01502 | 1.44 |
| 13.2 | | | 0.01776 | 0.01680 | 1.44 |
| 14 | | | 0.01739 | 0.01851 | 1.44 |

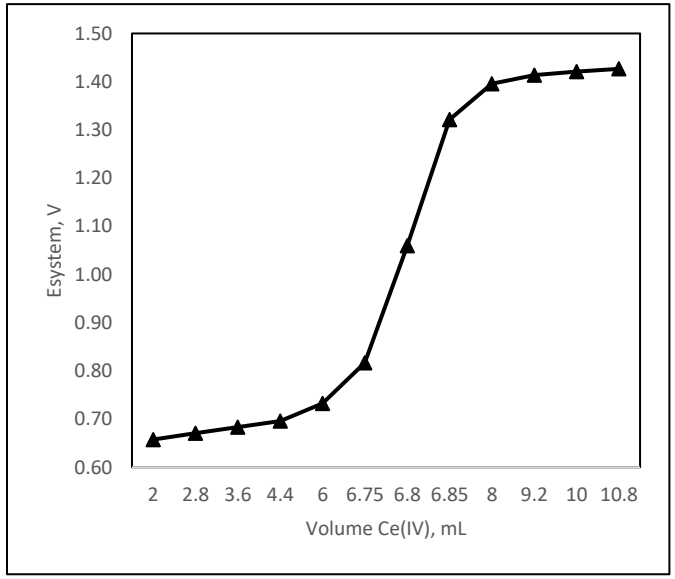


***Figure 6-1 Redox titration curve showing the logarithmic relationship: potential vs analyte concentration.***

*Table 6-2 Mean error and Standard deviation of Iron(II) determination in aqueous $H_2SO_4$-$Fe_2(SO_4)_3$-$FeSO_4$-$H_2O$ solution at 3 g/L total Iron.*

| Temp. ℃ | Fe(III)/Fe(II) | Initial Fe (g/L) | | Fe Found (g/L) | | Error (g/L) | |
|---|---|---|---|---|---|---|---|
| | | Fe (III) | Fe (II) | Fe (III) | Fe (II) | Fe (III) | Fe (II) |
| **25** | 0.1 | 0.27 | 2.7 | - | 2.68 | - | 0.02 |
| **35** | 0.1 | 0.27 | 2.7 | - | 2.50 | - | 0.20 |
| **45** | 0.1 | 0.27 | 2.7 | - | 2.68 | - | 0.02 |
| **55** | 0.1 | 0.27 | 2.7 | - | 2.64 | - | 0.06 |
| **60** | 0.1 | 0.27 | 2.7 | - | 2.59 | - | 0.11 |
| **65** | 0.1 | 0.27 | 2.7 | - | 2.68 | - | 0.02 |
| **70** | 0.1 | 0.27 | 2.7 | - | 2.70 | - | 0.00 |
| **Mean error: Fe(II) = ±0.06; Standard deviation: Fe(II) = ± 0.07** | | | | | | | |
| **25** | 0.5 | 1 | 2 | - | 2.01 | - | 0.01 |
| **35** | 0.5 | 1 | 2 | - | 2.06 | - | 0.06 |
| **45** | 0.5 | 1 | 2 | - | 2.04 | - | 0.04 |
| **55** | 0.5 | 1 | 2 | - | 2.01 | - | 0.01 |
| **60** | 0.5 | 1 | 2 | - | 2.10 | - | 0.10 |
| **65** | 0.5 | 1 | 2 | - | 2.08 | - | 0.08 |
| **70** | 0.5 | 1 | 2 | - | 2.10 | - | 0.10 |
| **Mean error: Fe(II) = ±0.06; Standard deviation: Fe(II) = ± 0.04** | | | | | | | |
| **25** | 1 | 1.5 | 1.5 | - | 1.56 | - | 0.06 |
| **35** | 1 | 1.5 | 1.5 | - | 1.45 | - | 0.05 |
| **45** | 1 | 1.5 | 1.5 | - | 1.56 | - | 0.06 |
| **55** | 1 | 1.5 | 1.5 | - | 1.56 | - | 0.06 |
| **60** | 1 | 1.5 | 1.5 | - | 1.59 | - | 0.09 |
| **65** | 1 | 1.5 | 1.5 | - | 1.45 | - | 0.05 |
| **70** | 1 | 1.5 | 1.5 | - | 1.45 | - | 0.05 |
| **Mean error: Fe(II) = ±0.03; Standard deviation: Fe(II) = ± 0.02** | | | | | | | |
| **25** | 2 | 2 | 1 | - | 1.03 | - | 0.03 |
| **35** | 2 | 2 | 1 | - | 1.07 | - | 0.07 |
| **45** | 2 | 2 | 1 | - | 1.03 | - | 0.03 |
| **55** | 2 | 2 | 1 | - | 1.05 | - | 0.05 |
| **60** | 2 | 2 | 1 | - | 1.03 | - | 0.03 |
| **65** | 2 | 2 | 1 | - | 1.01 | - | 0.01 |
| **70** | 2 | 2 | 1 | - | 1.03 | - | 0.03 |
| **Mean error: Fe(II) = ±0.06; Standard deviation: Fe(II) = ± 0.01** | | | | | | | |
| **25** | 10 | 2.7 | 0.27 | - | 0.36 | - | 0.09 |
| **35** | 10 | 2.7 | 0.27 | - | 0.31 | - | 0.04 |
| **45** | 10 | 2.7 | 0.27 | - | 0.29 | - | 0.02 |
| **55** | 10 | 2.7 | 0.27 | - | 0.29 | - | 0.02 |
| **60** | 10 | 2.7 | 0.27 | - | 0.27 | - | 0.00 |
| **65** | 10 | 2.7 | 0.27 | - | 0.28 | - | 0.01 |
| **70** | 10 | 2.7 | 0.27 | - | 0.28 | - | 0.01 |
| **Mean error: Fe(II) = ±0.03; Standard deviation: Fe(II) = ± 0.03** | | | | | | | |

*Table 6-3 Mean error and Standard deviation of Iron(II) determination in aqueous $H_2SO_4$-$Fe_2(SO_4)_3$-$FeSO_4$-$H_2O$ solution at 6 g/L total Iron*

| Temp. ℃ | Fe(III)/Fe(II) | Initial Fe (g/L) | | Fe Found (g/L) | | Error (g/L) | |
|---|---|---|---|---|---|---|---|
| | | Fe (III) | Fe (II) | Fe (III) | Fe (II) | Fe (III) | Fe (II) |
| **25** | 0.01 | 0.0594 | 5.94 | - | 6.03 | - | 0.09 |
| **35** | 0.01 | 0.0594 | 5.94 | - | 6.01 | - | 0.07 |
| **45** | 0.01 | 0.0594 | 5.94 | - | 5.92 | - | 0.02 |
| **55** | 0.01 | 0.0594 | 5.94 | - | 5.96 | - | 0.02 |
| **60** | 0.01 | 0.0594 | 5.94 | - | 5.96 | - | 0.02 |
| **65** | 0.01 | 0.0594 | 5.94 | - | 6.03 | - | 0.09 |
| **70** | 0.01 | 0.0594 | 5.94 | - | 5.92 | - | 0.02 |
| **Mean error: Fe(II) = ±0.05; Standard deviation: Fe(II) = ± 0.03** | | | | | | | |
| **25** | 0.2 | 1 | 5 | - | 4.95 | - | 0.05 |
| **35** | 0.2 | 1 | 5 | - | 4.95 | - | 0.05 |
| **45** | 0.2 | 1 | 5 | - | 5.28 | - | 0.28 |
| **55** | 0.2 | 1 | 5 | - | 5.28 | - | 0.28 |
| **60** | 0.2 | 1 | 5 | - | 5.28 | - | 0.28 |
| **65** | 0.2 | 1 | 5 | - | 5.03 | - | 0.03 |
| **70** | 0.2 | 1 | 5 | - | 5.28 | - | 0.28 |
| **Mean error: Fe(II) = ±0.18; Standard deviation: Fe(II) = ± 0.12** | | | | | | | |
| **25** | 5 | 5 | 1 | - | 1.03 | - | 0.03 |
| **35** | 5 | 5 | 1 | - | 0.98 | - | 0.02 |
| **45** | 5 | 5 | 1 | - | 1.01 | - | 0.01 |
| **55** | 5 | 5 | 1 | - | 1.01 | - | 0.01 |
| **60** | 5 | 5 | 1 | - | 1.03 | - | 0.03 |
| **65** | 5 | 5 | 1 | - | 1.01 | - | 0.01 |
| **70** | 5 | 5 | 1 | - | 1.01 | - | 0.01 |
| **Mean error: Fe(II) = ±0.01; Standard deviation: Fe(II) = ± 0.01** | | | | | | | |
| **25** | 100 | 5.94 | 0.0594 | - | 0.058 | - | 0.001 |
| **35** | 100 | 5.94 | 0.0594 | - | 0.063 | - | 0.003 |
| **45** | 100 | 5.94 | 0.0594 | - | 0.058 | - | 0.001 |
| **55** | 100 | 5.94 | 0.0594 | - | 0.060 | - | 0.001 |
| **60** | 100 | 5.94 | 0.0594 | - | 0.061 | - | 0.002 |
| **65** | 100 | 5.94 | 0.0594 | - | 0.063 | - | 0.003 |
| **70** | 100 | 5.94 | 0.0594 | - | 0.060 | - | 0.001 |
| **Mean error: Fe(II) = ±0.002; Standard deviation: Fe(II) = ± 0.001** | | | | | | | |

*Table 6-4 Mean error and Standard deviation of Iron(II) determination in aqueous $CuSO_4$-$H_2SO_4$-$Fe_2(SO_4)_3$-$FeSO_4$-$H_2O$ solution*

| Temp. ℃ | $Cu^{2+}$ (g/L) | Fe(III)/Fe(II) | Initial Fe (g/L) | | Fe Found (g/L) | | Error (g/L) | |
|---|---|---|---|---|---|---|---|---|
| | | | Fe (III) | Fe (II) | Fe (III) | Fe (II) | Fe (III) | Fe (II) |
| **25** | 40 | 0.2 | 0.5 | 2.5 | - | 2.52 | - | 0.02 |
| **35** | 40 | 0.2 | 0.5 | 2.5 | - | 2.52 | - | 0.02 |
| **45** | 40 | 0.2 | 0.5 | 2.5 | - | 2.52 | - | 0.02 |
| **55** | 40 | 0.2 | 0.5 | 2.5 | - | 2.57 | - | 0.07 |
| **60** | 40 | 0.2 | 0.5 | 2.5 | - | 2.52 | - | 0.02 |
| **65** | 40 | 0.2 | 0.5 | 2.5 | - | 2.52 | - | 0.02 |
| **70** | 40 | 0.2 | 0.5 | 2.5 | - | 2.57 | - | 0.07 |
| **Mean error: Fe(II) = ±0.04 ; Standard deviation: Fe(II) = ± 0.02** | | | | | | | | |
| **25** | 36 | 2 | 4 | 2 | - | 2.03 | - | 0.03 |
| **35** | 36 | 2 | 4 | 2 | - | 2.06 | - | 0.06 |
| **45** | 36 | 2 | 4 | 2 | - | 2.06 | - | 0.06 |
| **55** | 36 | 2 | 4 | 2 | - | 2.04 | - | 0.04 |
| **60** | 36 | 2 | 4 | 2 | - | 2.06 | - | 0.06 |
| **65** | 36 | 2 | 4 | 2 | - | 2.04 | - | 0.04 |
| **70** | 36 | 2 | 4 | 2 | - | 2.04 | - | 0.04 |
| **Mean error: Fe(II) = ±0.05; Standard deviation: Fe(II) = ± 0.008** | | | | | | | | |
| **25** | 45 | 2 | 2 | 1 | - | 1.03 | - | 0.03 |
| **35** | 45 | 2 | 2 | 1 | - | 1.01 | - | 0.01 |
| **45** | 45 | 2 | 2 | 1 | - | 1.03 | - | 0.03 |
| **55** | 45 | 2 | 2 | 1 | - | 1.01 | - | 0.01 |
| **60** | 45 | 2 | 2 | 1 | - | 1.03 | - | 0.03 |
| **65** | 45 | 2 | 2 | 1 | - | 1.01 | - | 0.01 |
| **70** | 45 | 2 | 2 | 1 | - | 1.02 | - | 0.02 |
| **Mean error: Fe(II) = ±0.02; Standard deviation: Fe(II) = ± 0.01** | | | | | | | | |
| **25** | 50 | 2 | 2 | 1 | - | 1.05 | - | 0.05 |
| **35** | 50 | 2 | 2 | 1 | - | 1.04 | - | 0.04 |
| **45** | 50 | 2 | 2 | 1 | - | 1.04 | - | 0.04 |
| **55** | 50 | 2 | 2 | 1 | - | 1.01 | - | 0.01 |
| **60** | 50 | 2 | 2 | 1 | - | 1.05 | - | 0.05 |
| **65** | 50 | 2 | 2 | 1 | - | 1.04 | - | 0.04 |
| **70** | 50 | 2 | 2 | 1 | - | 1.01 | - | 0.01 |
| **Mean error: Fe(II) = ±0.03; Standard deviation: Fe(II) = ± 0.02** | | | | | | | | |
| **25** | 36 | 5 | 2 | 0.4 | - | 0.39 | - | 0.01 |
| **35** | 36 | 5 | 2 | 0.4 | - | 0.39 | - | 0.01 |
| **45** | 36 | 5 | 2 | 0.4 | - | 0.38 | - | 0.02 |
| **55** | 36 | 5 | 2 | 0.4 | - | 0.38 | - | 0.02 |
| **60** | 36 | 5 | 2 | 0.4 | - | 0.40 | - | 0.00 |
| **65** | 36 | 5 | 2 | 0.4 | - | 0.39 | - | 0.01 |
| **70** | 36 | 5 | 2 | 0.4 | - | 0.38 | - | 0.02 |
| **Mean error: Fe(II) = ±0.01; Standard deviation: Fe(II) = ± 0.007** | | | | | | | | |
| **25** | 40 | 10 | 2 | 0.2 | - | 0.21 | - | 0.01 |
| **35** | 40 | 10 | 2 | 0.2 | - | 0.21 | - | 0.01 |
| **45** | 40 | 10 | 2 | 0.2 | - | 0.22 | - | 0.02 |
| **55** | 40 | 10 | 2 | 0.2 | - | 0.22 | - | 0.02 |
| **60** | 40 | 10 | 2 | 0.2 | - | 0.22 | - | 0.02 |
| **65** | 40 | 10 | 2 | 0.2 | - | 0.20 | - | 0.00 |
| **70** | 40 | 10 | 2 | 0.2 | - | 0.22 | - | 0.02 |
| **Mean error: Fe(II) = ±0.02; Standard deviation: Fe(II) = ± 0.008** | | | | | | | | |
| **25** | 45 | 10 | 5.45 | 0.545 | - | 0.56 | - | 0.01 |
| **35** | 45 | 10 | 5.45 | 0.545 | - | 0.54 | - | 0.01 |
| **45** | 45 | 10 | 5.45 | 0.545 | - | 0.56 | - | 0.01 |
| **55** | 45 | 10 | 5.45 | 0.545 | - | 0.56 | - | 0.01 |
| **60** | 45 | 10 | 5.45 | 0.545 | - | 0.57 | - | 0.02 |
| **65** | 45 | 10 | 5.45 | 0.545 | - | 0.57 | - | 0.02 |
| **70** | 45 | 10 | 5.45 | 0.545 | - | 0.56 | - | 0.01 |
| **Mean error: Fe(II) = ±0.02; Standard deviation: Fe(II) = ± 0.006** | | | | | | | | |

## 6.3 Summary

As we discussed, the potentiometric titration of the $H_2SO_4$-$Fe_2(SO_4)_3$-$FeSO_4$-$H_2O$ and the $CuSO_4$-$H_2SO_4$-$Fe_2(SO_4)_3$-$FeSO_4$-$H_2O$ systems allowed for a high precision determination of the ferrous iron. The measured values shown in table 6-1 under all nominal $Fe^{3+}/Fe^{2+}$ ratios of which the synthetic solutions were subjected to are in well agreement with those initial values of when each fresh solution was prepared. The average percent error of the assays at temperatures from 25 to 70℃ and nominal $Fe^{3+}/Fe^{2+}$ ratios of 100:1, 10:1, 5:1, 2:1, 1:1, 1:2, 1:5, 1:10 and 1:100 is of 2.53%, which means an average difference of around 0.00025 mol/L between the initial values and the results of the titration assays. Although higher averages of 3.8% and 3.5% were observed at temperatures of 35 and 60℃, as well as averages of 3.9% and 3.4% at nominal ratios of 1:1 and 2:1, no real relationship was found among these. Tables 6-2, 6-3 show the mean error and standard deviations of each assay under specific nominal $Fe^{3+}/Fe^{2+}$ ratio, temperature, and concentrations of ferric and ferrous species in the $H_2SO_4$-$Fe_2(SO_4)_3$-$FeSO_4$-$H_2O$. Similarly, Table 6-3 show the mean error and standard deviation of each assay under the above-mentioned parameters in addition to cupric ions concentration in the $CuSO_4$-$H_2SO_4$-$Fe_2(SO_4)_3$-$FeSO_4$-$H_2O$.

These findings further support the validity of the equation (1.1) developed by Yue et al. to predict the redox potential of the aqueous $H_2SO_4$-$Fe_2(SO_4)_3$-$FeSO_4$-$H_2O$ system over a broad range nominal $Fe^{3+}/Fe^{2+}$ ratios and temperatures. Furthermore, these findings expand the applicability of Yue's model to determine ferric and ferrous concentrations based on the prediction of the redox potential, offering an alternative to volumetric methods typically employed for ferric and ferrous determination.

# 7 Electrochemical Analysis of Current Efficiency Loss by Iron

## 7.1 Introduction

Current efficiency is evaluated in this work as a function of Iron(III) and Cu(II) ions concentrations as expressed by Khouraibchia and Moats (2009, 2010) according to the following:

$$\xi(\%) = 88.19 - 4.91[Fe^{3+}] + 0.52[Cu^{2+}] + 1.81 \times 10^{-3} j - 6.83 \times 10^{-3}[Cu^{2+}]^2 + 0.028[Fe^{3+}][Cu^{2+}] + 4.015 \times 10^{-3} j[Fe^{3+}] \quad (2.12)$$

It is well known that current efficiency increases with increasing current density and increasing concentrations of copper and sulfuric acid in the electrolyte, but decreases with increasing $Fe^{3+}$ concentration and temperature [7, 8, 13, 33, 37]. The rate of reduction of the $Fe^{3+}$ is limited by the mass transport of these ions to the cathode surface while the rate determining step for copper deposition is typically charge transfer. Thus, iron reduction occurs at its limiting current density, and copper reduction does not. Therefore, in the absence of inefficiencies, when $Fe^{3+}$ is present the cathode current efficiency is determined by the diffusion of $Fe^{3+}$ to the cathode [2, 34, 42].

Two industrial solutions employed in electrowinning and electrorefining are evaluated in terms of composition, temperature and reported current efficiencies to allow for a comparison of the synthetic solutions prepared in this study and thus evaluate the current efficiency of these solutions. As it may be notice, assumptions are theoretical values are applied as needed in the comparison of these solutions in attempt to establish a true relationship among solutions and allow for the application of Khouraibchia's & Moats equation.

## 7.2 Results and Discussion

The following data presents a comparison of the synthetic solutions prepared in this work to one electrorefining solution and one electrowinning solution currently employed in industry provided by Freeport Mcmoran Inc. Table 7-1 shows the chemical composition of both solutions. As can be seen, sulfuric acid concentration is in the range of 190 to 200 g/L in two solutions, and iron concentration is around the 2.5 g/L and 1.8 g/L in ER and EW electrolytes, respectively. The two electrolytes are compared further in table 7-2 with synthetic electrolytes prepared in this work as a function of nominal $Fe^{3+}/Fe^{2+}$ ratio, temperature and observed potential.

As stated in the introduction, theoretical values from literature and calculated values are used in an effort to establish a relationship between the industrial solutions with the synthetic prepared in this work, to further evaluate current efficiency in terms of the CE equation (2.12).

***Table 7-1 Composition in copper electrolytes employed in copper electrowinning and electrorefining***

| **Composition of Industrial Copper Electrolytes** | | |
|---|---|---|
| **Component** | **Electrorefining** | **Electrowinning** |
| Sulfuric Acid | 190 - 200 g/L | 190-200 g/L |
| Cu | 40 - 45 g/L | 31-36 g/L |
| $Cl^-$ | 0.03 - 0.04 g/L | 15-20 g/L |
| As | 5.5 - 6.5 g/L | - |
| Bi | 0.11 - 0.12 g/L | - |
| Ca | 0.52 - 0.58 g/L | - |
| Fe | 2.2 - 2.7 g/L | 1.2 – 2.5 g/L |
| Mg | 0.27 - 0.3 g/L | - |
| Na | 2.8 - 3.3 g/L | - |
| Ni | 16.2 - 19 g/L | - |
| Sb | 0.22 - 0.26 g/L | - |
| Co | - | 0.18-0.22 g/L |
| Mn | - | 0.025-0.030 g/L |
| Temperature | 67°C | 40°C |

The following is the applied procedure to account for the unknown values as shown in table 7-2; a nominal ferric/ferrous ratio for the ER solution is obtained through temperature, total iron concentration and observed potential in solution; overall ORP of ER and EW solutions is obtained via Yue's equation (2.7); current efficiencies for synthetic solutions are obtained via equation (2.12) through a correlation between nominal ferric/ferrous ratio, ferric concentration, cupric concentration and theoretical current densities between the three solutions.

***Table 7-2 Comparison of electrolytes based on nominal $Fe^{3+}/Fe^{2+}$, temperature and $E_{obs}$***

| | **Temp. (°C)** | **$Cu^{2+}$ (g/L)** | **Total Fe (g/L)** | **Nominal $Fe^{3+}/Fe^{2+}$ Ratio** | **$E_{obs}$ (mV)** | **$E_{SHE}$ [Equation] (mV)** | **Current Density ($Amp/m^2$)** | **Current Efficiency** |
|---|---|---|---|---|---|---|---|---|
| **Electrorefining (67°C)** | 65 | 45 | 2.45 | - | 385 | 549.7 | 400 | 89.6 % |
| | 70 | 45 | 2.45 | - | 385 | 545.5 | 400 | 89.6% |
| **Electrowinning (40°C)** | 35 | 35 | 1.65 | 4:1 | 531* | 714.3 | 350 | 91.8% |
| | 45 | 35 | 1.65 | 4:1 | 543* | 718.3 | 350 | 91.8% |
| **Synthetic Solutions** | 65 | 45 | 6 | 1:100 | 387 | 551.4 | - | - |
| | 45 | 36 | 6 | 1:100 | 372 | 553.6 | - | - |
| | 65 | 45 | 2.4 | 4:1 | 561* | 725.8 | - | - |
| | 45 | 36 | 2.4 | 4:1 | 543* | 724.4 | - | - |

***** Theoretical value

Results of the theoretical correlation between ER, EW and synthetic solutions prepared in this study based on nominal ferric/ferrous ratio, ferric iron concentration, cupric concentration, total iron concentration and current efficiency are shown in figure 7-3. In the ER electrolyte, lower and upper-end total iron concentrations according to table 7-1 are considered and plotted against reported current density of 400 $A/m^2$ and cupric concentrations of 40-45 g/L. A nominal ferric/ferrous ratio of 1:100 is first plotted based on the observed potential of 385.1 mV of the solution.

***Table 7-3 Theoretical current efficiencies of the ER, EW and synthetic electrolytes based on Khouraibchia & Moats model***

| | C.D. ($A/m^2$) | Cu2+ (g/L) | $Fe^{3+}$ (g/L) | Current Efficiency (%) | Nominal $Fe^{3+}/Fe^{2+}$ | Total Fe (g/L) |
|---|---|---|---|---|---|---|
| **Electrorefining** | 400 | 45 | 0.027 | 98.428 | 0.01 | 2.7 |
| | 400 | 40 | 2.426 | 93.488 | 100 | 2.4 |
| **Electrowinning** | 350 | 36 | 2 | 93.698 | 4 | 2.5 |
| | 350 | 31 | 1 | 95.743 | 5 | 1.2 |
| **Synthetic electrolytes** | 400 | 45 | 5.46 | 87.325 | 10 | 6.0 |
| | 400 | 40 | 0.055 | 98.667 | 0.1 | 6.0 |
| | 350 | 36 | 2.5 | 92.450 | 5 | 3.0 |
| | 350 | 31 | 2.7 | 91.261 | 10 | 3.0 |

However, as can be noticed, theoretical current efficiency via equation (2.12) is significantly higher than that reported by industry, of about 90% and 98%, respectively. A second approach was made with lower cupric and iron concentration of 40 g/L and 2.4, respectively and according to table 7-1, where a nominal ratio of 100:1 was found to be closer to the current efficiency reported, of 93.5 and 90%, respectively. The EW solution was also plotted to its lower and upper-end values for cupric and iron concentration. As shown in table 7-3, the reported CE values from the nominal ferric/ferrous ratios values are within a 1.7% and 3.7% difference from those calculated from equation (2.12). Lastly, 4 synthetic solutions are compared in terms of nominal ferric/ferrous ratio and current efficiency similarities. As can be seen, CE calculated values from nominal ratios of 5 and 10 are in well agreement with CE values reported from industry and are dependent on total iron concentration. These results allowed to apply a theoretical current efficiency to synthetic electrolytes very close in range with CE values obtained from industry, however, a more detail, complete study is necessary in order to establish a real relationship within the sulfates concentrations, nominal ferric/ferrous ratio and current efficiency. It is imperative to quantify iron species, cupric ions, current density, temperature and ORP values for a successful evaluation.

## 7.3 Summary

Theoretical CE values obtained via equation (2.12) and applied to synthetic solutions prepared in this work showed small variances from those values reported by the industry. This is due to the lack of complete data such as the nominal ferric/ferrous ratio in the electrorefining electrolyte and ORP values from both electrolytes. Although the calculated values from EW solutions and synthetic electrolytes of nominal ratio of 5 and 10 are in agreement with real CE values, no real assumption can be made regarding a true relationship within solutions. A complete study accounting for nominal ratios in solutions, redox potential values and temperatures is necessary in order to establish a true relationship. This with the purpose to obtain a real current efficiency factor via Eq. (2.7), where a nominal ferric/ferrous ratio dependent on temperature and total iron concentration will be able to determine this factor.

# 8 Conclusions and Summary

The applicability of Eq. (2.7) in the aqueous $H_2SO_4$-$Fe_2(SO_4)_3$-$FeSO_4$-$H_2O$ and $H_2SO_4$-$CuSO_4$-$Fe_2(SO_4)_3$-$FeSO_4$-$H_2O$ systems is validated over a wide range of temperatures and sulfate concentrations. The model is validated under nominal ferric/ferrous ratios from 0.01 to 100, from temperatures from 25 to 70°C, concentrations of cupric ion from 35 to 50 g/L, total iron from 1 to 6 g/L and sulfuric acid from 170-200 g/L. Its applicability was expanded to higher concentrations of iron (up to 6 g/L) and copper (up to 50 g/L). It was observed that Cu ions in concentrations range of 35 to 50 g/L exerted no significant effect on the prediction accuracy of the Eq. (2.7) model.

Moreover, the applicability of this equation is expanded to the accurate determination of ferrous and ferric iron concentrations in the above-mentioned systems based on the measured redox potential, temperature and total iron concentration, providing an alternative to complicated volumetric methods for ferrous and ferric determination. Results from the potentiometric determination of iron(II) concentrations in synthetic solutions showed a percent error average of 2.53% from initial concentrations, which further support the validity of the equation (2.7) developed by Yue et al. to predict the redox potential of the aqueous $H_2SO_4$-$Fe_2(SO_4)_3$-$FeSO_4$-$H_2O$ system over a broad range nominal $Fe^{3+}/Fe^{2+}$ ratios and temperatures mentioned previously.

Finally, presumable results of the evaluation of current efficiency via Eq. (2.12) to establish a relationship with Eq. (2.7) by comparing two industrial electrolytes, one for electrorefining and one for electrowinning, with several synthetic solutions presented in this work showed significant differences between current efficiencies (measured vs Eq. 2.7) at each solution.

More in-situ data as far as total iron concentration, nominal ferric/ferrous ratio and cupric ions is needed for a complete study to provide a real relationship between Eq. (2.7) and Eq. (2.12). Further industrial data will be investigated to support this method to apply Eq. (2.7) for the direct calculation of current efficiency.

# References


[1] M. E. Schlesinger, M. J. King, K. C. Sole, and W. G. Davenport, *Extractive Metallurgy of Copper*, Fifth. 2011.

[2] M. Moats and Y. Khouraibchia, "Effective diffusivity of ferric ions and current efficiency in stagnant synthetic copper electrowinning solutions," *Miner. Metall. Process.*, vol. 26, no. 4, pp. 179–186, 2009.

[3] E. Rudnik and N. Dashbold, "Study on copper recovery from smelted low-grade e-scrap using hydrometallurgical methods," *Miner. Metall. Process.*, vol. 34, no. 1, pp. 20–29, 2017.

[4] Y. Gendel and O. Lahav, "Accurate determination of Fe(II) concentrations in the presence of a very high soluble Fe(III) background," *Appl. Geochemistry*, vol. 23, no. 8, pp. 2123–2129, 2008.

[5] T. T. Chen and J. E. Dutrizac, "The mineralogy of copper electrorefining," *Jom*, vol. 42, no. 8, pp. 39–44, 1990.

[6] J. E. Dutrizac, "The kinetics of dissolution of chalcopyrite in ferric ion media," *Metall. Trans. B*, vol. 9, no. 4, pp. 431–439, 1978.

[7] G. Yue, L. Zhao, O. G. Olvera, and E. Asselin, "Speciation of the H2SO4-Fe2(SO 4)3-FeSO4-H2O system and development of an expression to predict the redox potential of the Fe3 +/Fe 2 + couple up to 150 °c," *Hydrometallurgy*, vol. 147–148, pp. 196–209, 2014.

[8] T. Kalliomäki, J. Aromaa, and M. Lundström, "Modeling the effect of composition and temperature on the conductivity of synthetic copper electrorefining electrolyte," *Minerals*, vol. 6, no. 3, 2016.

[9] T. Kalliomaki, "EFFECT OF COMPOSITION AND TEMPERATURE ON PHYSICO-CHEMICAL PROPERTIES OF COPPER ELECTROLYTE," 2015.

[10] M. Free *et al.*, “Electrometallurgy-Now and in the Future,” pp. 1–25, 1955.

[11] A. P. Brown, R. O. Loutfy, G. M. Cook, and N. P. Yao, “The Electrorefining of Copper from a Cuprous Ion Complexing Electrolyte,” *JOM J. Miner. Met. Mater. Soc.*, vol. 33, no. 7, pp. 49–57, 1981.

[12] I. Lehtiniemi *et al.*, “Validation of electrolyte conductivity models in industrial copper electrorefining,” *Miner. Metall. Process.*, vol. 35, no. 3, pp. 117–124, 2018.

[13] S. Gürmen, G. Orhan, C. Arslan, and S. Timur, “Copper refining electrolysis at high current densities,” *ARI Bull. Istanbul Tech. Univ.*, vol. 54, no. 2, pp. 40–44, 2004.

[14] A. J. Bard and L. R. Faulkner, *Fundamentals and Applications*, vol. 30. 1980.

[15] M. J. Nicol, “Electrowinning and Electrorefining of Electrowinning and Electrorefining of Copper”, 2008.

[16] J. M. Casas, G. Crisóstomo, and L. Cifuentes, “Speciation of the Fe(II)–Fe(III)–H2SO4–H2O system at 25 and 50 °C,” *Hydrometallurgy*, vol. 80, no. 4, pp. 254–264, 2005.

[17] E. Mostad, S. Rolseth, and J. Thonstad, “Electrowinning of iron from sulphate solutions,” *Hydrometallurgy*, vol. 90, no. 2–4, pp. 213–220, 2008.

[18] C. G. Anderson, “Optimization of industrial copper electrowinning solutions,” *IMPC 2016 - 28th Int. Miner. Process. Congr.*, vol. 2016-Septe, no. 1, pp. 1–3, 2016.

[19] G. Yue, “Speciation of the sulfuric acid-ferric sulfate-ferrous sulfate-water system and its application to chalcopyrite leaching kinetics up to 150 $^{o}$C,” no. March, 2015.

[20] R. Al Shakarji, Y. He, and S. Gregory, “Statistical analysis of the effect of operating parameters on acid mist generation in copper electrowinning,” *Hydrometallurgy*, vol. 106, no. 1–2, pp. 113–118, 2011.

[21] P. Laforest, “Understanding Impurities in copper electrometallurgy,” 2015.

[22] L. Cifuentes, J. M. Casas, P. Consulting, and J. Simpson, “TEMPERATURE

DEPENDENCE OF THE SPECIATION OF," no. December 2017, 2006.

[23] G. Yue and E. Asselin, "Kinetics of ferric ion reduction on chalcopyrite and its influence on leaching up to 150 °c," *Electrochim. Acta*, vol. 146, pp. 307–321, 2014.

[24] J. M. Casas, P. Consulting, and L. Cifuentes, "Speciation of the Fe(II)-Fe(III)-H2SO4-H 2O system at 25 and 50 °c," no. December 2017, 2005.

[25] V. Tjandrawan, "The role of manganese in the electrowinning of copper and zinc," pp. 1, 8, 2010.

[26] G. Yue, A. G. Guezennec, and E. Asselin, "Extended validation of an expression to predict ORP and iron chemistry: Application to complex solutions generated during the acidic leaching or bioleaching of printed circuit boards," *Hydrometallurgy*, vol. 164, pp. 334–342, 2016.

[27] K. S. Pitzer, R. N. Roy, and L. F. Silvester, "Thermodynamics of Electrolytes. 7. Sulfuric Acid," *J. Am. Chem. Soc.*, vol. 99, no. 15, pp. 4930–4936, 1977.

[28] L. Cifuentes, R. Ortiz, and J. M. Casas, "Electrowinning of copper in a lab-scale squirrel-cage cell with anion membrane," *AIChE J.*, vol. 51, no. 8, pp. 2273–2284, 2005.

[29] Cifuentes, L., Glasner, R., Crisostomo, G., Casas, J.M., Simpson, J., "Aspects of the Development of a New Copper Electrowinning Cell based on Reactive Electrodialysis," vol. 147, no. 2, pp. 347–348, 2001.

[30] L. Cifuentes and J. Simpson, "Temperature dependence of the cathodic and anodic kinetics in a copper electrowinning cell based on reactive electrodialysis," *Chem. Eng. Sci.*, vol. 60, no. 17, pp. 4915–4923, 2005.

[31] J. M. Casas, G. Crisóstomo, and L. Cifuentes, "Dissolution of metallic copper in aqueous sulphuric acid - Ferric sulphate solutions," *Can. Metall. Q.*, vol. 45, no. 3, pp. 243–248, 2006.

[32] J. L. Owings, “The Effect of Ferric Iron Upon the Current Efficiency and the Deposition of Copper in the Electrowinning of Copper from Copper Sulphate Solutions,” no. 1952, 1970.

[33] E. L. Cussler, *Diffusion Mass Transfer in Fluid Systems*, 3rd ed. Cambridge University Press, 2009.

[34] G. Cifuentes, J. Simpson, F. Lobos, L. Briones, and A. Morales, “An alternative copper electrowinning process based on reactive electrodialysis (RED),” *Chem. Eng. Trans.*, vol. 19, pp. 157–162, 2010.

[35] P. Sandoval, Scot P., Robinson, Timothy G., Cook, “Method and apparatus for electrowinning copper using the ferrous/ferric anode reaction,” 2008.

[36] N. J. Aslin and W. Webb, “Current distribution in modern copper refining.”

[37] B. Panda and S. C. Das, “Electrowinning of copper from sulfate electrolyte in presence of sulfurous acid,” *Hydrometallurgy*, vol. 59, no. 1, pp. 55–67, 2001.

[38] M. J. Nicol and I. Lázaro, “The role of EH measurements in the interpretation of the kinetics and mechanisms of the oxidation and leaching of sulphide minerals,” *Hydrometallurgy*, vol. 63, no. 1, pp. 15–22, 2002.

[39] M. S. Moats, A. Luyima, and W. Cui, “Examination of copper electrowinning smoothing agents. Part I: A review,” *Miner. Metall. Process.*, vol. 33, no. 1, pp. 7–13, 2016.

[40] J. Zhu, X. Yang, F. Fan, and Y. Li, “Factors affecting the determination of iron species in the presence of ferric iron,” *Appl. Water Sci.*, vol. 8, no. 8, pp. 1–4, 2018.

[41] H. Tamura, K. Goto, T. Yotsuyanagi, and M. Nagayama, “Spectrophotometric determination of iron(II) with 1,10-phenanthroline in the presence of large amounts of iron(III),” *Talanta*, vol. 21, no. 4, pp. 314–318, 1974.

[42] N. Hiroyoshi, H. Miki, T. Hirajima, and M. Tsunekawa, “Enhancement of chalcopyrite leaching by ferrous ions in acidic ferric sulfate solutions,” *Hydrometallurgy*, vol. 60, no. 3,

pp. 185–197, 2001.

[43] N. Hiroyoshi, M. Arai, H. Miki, M. Tsunekawa, and T. Hirajima, “A new reaction model for the catalytic effect of silver ions on chalcopyrite leaching in sulfuric acid solutions,” *Hydrometallurgy,* vol. 63, no. 3, pp. 257–267, 2002.

[44] N. Hiroyoshi, H. Kitagawa, and M. Tsunekawa, “Effect of solution composition on the optimum redox potential for chalcopyrite leaching in sulfuric acid solutions,” *Hydrometallurgy,* vol. 91, no. 1–4, pp. 144–149, 2008.

[45] D. H. Angell and T. Dickinson, “The kinetics of the ferrous/ferric and ferro/ferricyanide reactions at platinum and gold electrodes. Part I. Kinetics at bare-metal surfaces,” *J. Electroanal. Chem.*, vol. 35, no. 1, pp. 55–72, 1972.

# Appendices

***Table A - 1 Results of the potentiometric titration of Fe(II) with Ce(IV) in the $H_2SO_4$-$Fe_2(SO_4)_3$-$FeSO_4$-$H_2O$ synthetic solution with a total of 3 g/L Iron.***

| Chemical Analysis | | Experimental results measured in the lab | | | | | | | | Calculated $Fe^{2+}$ amount by | | |
|---|---|---|---|---|---|---|---|---|---|---|---|---|
| Test | Assay | $Fe_{total}$ g/L | $Fe^{3+}$ g/L | $Fe^{2+}$ g/L | $Fe^{3+}/Fe^{2+}$ Nominal | $Cu^{2+}$ | T °C | $E_b$ (obs) mV | $E_{End}$ (End) mV | ΔV ml | V (Calc) g | Error % |
| 1 | 1 | 3 | 2 | 1 | 2:1 | - | 25 | 495.33 | 1060.33 | 4.6 | 1.0275 | 2.755 |
| | 2 | 3 | 2 | 1 | 2:1 | - | 35 | 506.68 | 1060.33 | 4.8 | 1.0722 | 7.222 |
| | 3 | 3 | 2 | 1 | 2:1 | - | 45 | 519.25 | 1060.33 | 4.6 | 1.0275 | 2.755 |
| | 4 | 3 | 2 | 1 | 2:1 | - | 55 | 531.83 | 1060.33 | 4.7 | 1.0499 | 4.989 |
| | 5 | 3 | 2 | 1 | 2:1 | - | 60 | 538.27 | 1060.33 | 4.6 | 1.0275 | 2.755 |
| | 6 | 3 | 2 | 1 | 2:1 | - | 65 | 545.32 | 1060.33 | 4.5 | 1.0052 | 0.521 |
| | 7 | 3 | 2 | 1 | 2:1 | - | 60 | 551.15 | 1060.33 | 4.6 | 1.0275 | 2.755 |
| 2 | 8 | 3 | 1 | 2 | 1:2 | - | 25 | 461.29 | 1060.33 | 9 | 2.0104 | 0.521 |
| | 9 | 3 | 1 | 2 | 1:2 | - | 35 | 473.25 | 1060.33 | 9.2 | 2.0551 | 2.755 |
| | 10 | 3 | 1 | 2 | 1:2 | - | 45 | 483.68 | 1060.33 | 9.15 | 2.0440 | 2.196 |
| | 11 | 3 | 1 | 2 | 1:2 | - | 55 | 490.12 | 1060.33 | 9 | 2.0104 | 0.521 |
| | 12 | 3 | 1 | 2 | 1:2 | - | 60 | 495.33 | 1060.33 | 9.4 | 2.0998 | 4.989 |
| | 13 | 3 | 1 | 2 | 1:2 | - | 65 | 501.46 | 1060.33 | 9.3 | 2.0774 | 3.872 |
| | 14 | 3 | 1 | 2 | 1:2 | - | 70 | 508.21 | 1060.33 | 9.4 | 2.0998 | 4.989 |
| 3 | 15 | 3 | 1.5 | 1.5 | 1:1 | - | 25 | 476.30 | 1060.33 | 6.5 | 1.4520 | 3.202 |
| | 16 | 3 | 1.5 | 1.5 | 1:1 | - | 35 | 487.74 | 1060.33 | 7 | 1.5637 | 4.244 |
| | 17 | 3 | 1.5 | 1.5 | 1:1 | - | 45 | 499.32 | 1060.33 | 7 | 1.5637 | 4.244 |
| | 18 | 3 | 1.5 | 1.5 | 1:1 | - | 55 | 512.51 | 1060.33 | 7 | 1.5637 | 4.244 |
| | 19 | 3 | 1.5 | 1.5 | 1:1 | - | 60 | 518.33 | 1060.33 | 7.1 | 1.5860 | 5.733 |
| | 20 | 3 | 1.5 | 1.5 | 1:1 | - | 65 | 526.61 | 1060.33 | 6.5 | 1.4520 | 3.202 |
| | 21 | 3 | 1.5 | 1.5 | 1:1 | - | 70 | 532.77 | 1060.33 | 6.5 | 1.4520 | 3.202 |
| 4 | 22 | 3 | 2.7 | 0.27 | 10:1 | - | 25 | 534.36 | 1060.33 | 1.6 | 0.3574 | 32.37 |
| | 23 | 3 | 2.7 | 0.27 | 10:1 | - | 35 | 546.24 | 1060.33 | 1.4 | 0.3127 | 15.83 |
| | 24 | 3 | 2.7 | 0.27 | 10:1 | - | 45 | 559.00 | 1060.33 | 1.3 | 0.2904 | 7.553 |
| | 25 | 3 | 2.7 | 0.27 | 10:1 | - | 55 | 572.68 | 1060.33 | 1.3 | 0.2904 | 7.553 |
| | 26 | 3 | 2.7 | 0.27 | 10:1 | - | 60 | 581.02 | 1060.33 | 1.2 | 0.2681 | 0.720 |
| | 27 | 3 | 2.7 | 0.27 | 10:1 | - | 65 | 588.47 | 1060.33 | 1.25 | 0.2792 | 3.417 |
| | 28 | 3 | 2.7 | 0.27 | 10:1 | - | 70 | 595.72 | 1060.33 | 1.25 | 0.2792 | 3.417 |
| 5 | 29 | 3 | 0.27 | 2.7 | 1:10 | - | 25 | 416.81 | 1060.33 | 12 | 2.6807 | 0.720 |
| | 30 | 3 | 0.27 | 2.7 | 1:10 | - | 35 | 424.48 | 1060.33 | 11.2 | 2.5012 | 7.339 |
| | 31 | 3 | 0.27 | 2.7 | 1:10 | - | 45 | 433.38 | 1060.33 | 12 | 2.6806 | 0.720 |
| | 32 | 3 | 0.27 | 2.7 | 1:10 | - | 55 | 445.64 | 1060.33 | 11.8 | 2.6359 | 2.375 |
| | 33 | 3 | 0.27 | 2.7 | 1:10 | - | 60 | 451.47 | 1060.33 | 11.6 | 2.5912 | 4.029 |
| | 34 | 3 | 0.27 | 2.7 | 1:10 | - | 65 | 455.15 | 1060.33 | 12 | 2.6806 | 0.720 |
| | 35 | 3 | 0.27 | 2.7 | 1:10 | - | 70 | 459.75 | 1060.33 | 12.1 | 2.7029 | 0.107 |

***Table A - 2 Results of the potentiometric titration of Fe(II) with Ce(IV) in the $H_2SO_4$-$Fe_2(SO_4)_3$-$FeSO_4$-$H_2O$ synthetic solution with a total of 6 g/L Iron.***

| Chemical Analysis | | Experimental results measured in the lab | | | | | | | | Calculated $Fe^{2+}$ amount by | | |
|---|---|---|---|---|---|---|---|---|---|---|---|---|
| Test | Assay | $Fe_{total}$ g/L | $Fe^{3+}$ g/L | $Fe^{2+}$ g/L | $Fe^{3+}/Fe^{2+}$ Nominal | $Cu^{2+}$ g/L | T °C | $E_b$ (obs) mV | $E_{End}$ (End) mV | ΔV ml | V (Calc) ml | Error % |
| 6 | 36 | 6 | 5 | 1 | 2:1 | - | 25 | 516.186 | 1060.33 | 4.2 | 1.0275 | 2.755 |
| | 37 | 6 | 5 | 1 | 2:1 | - | 35 | 528.454 | 1060.33 | 4.4 | 0.9829 | 1.713 |
| | 38 | 6 | 5 | 1 | 2:1 | - | 45 | 541.95 | 1060.33 | 4.5 | 1.0052 | 0.521 |
| | 39 | 6 | 5 | 1 | 2:1 | - | 55 | 555.445 | 1060.33 | 4.5 | 1.0052 | 0.521 |
| | 40 | 6 | 5 | 1 | 2:1 | - | 60 | 562.806 | 1060.33 | 4.6 | 1.0275 | 2.755 |
| | 41 | 6 | 5 | 1 | 2:1 | - | 65 | 569.553 | 1060.33 | 4.5 | 1.0052 | 0.521 |
| | 42 | 6 | 5 | 1 | 2:1 | - | 70 | 575.995 | 1060.33 | 4.5 | 1.0052 | 0.521 |
| 7 | 43 | 6 | 5.94 | .0594 | 100:1 | - | 25 | 594.396 | 1060.33 | 2.6 | 0.0581 | 2.224 |
| | 44 | 6 | 5.94 | .0594 | 100:1 | - | 35 | 608.505 | 1060.33 | 2.8 | 0.0626 | 5.297 |
| | 45 | 6 | 5.94 | .0594 | 100:1 | - | 45 | 624.76 | 1060.33 | 2.6 | 0.0581 | 2.224 |
| | 46 | 6 | 5.94 | .0594 | 100:1 | - | 55 | 641.629 | 1060.33 | 2.7 | 0.0603 | 1.536 |
| | 47 | 6 | 5.94 | .0594 | 100:1 | - | 60 | 646.843 | 1060.33 | 2.75 | 0.0614 | 3.417 |
| | 48 | 6 | 5.94 | .0594 | 100:1 | - | 65 | 655.124 | 1060.33 | 2.8 | 0.0625 | 5.297 |
| | 49 | 6 | 5.94 | .0594 | 100:1 | - | 70 | 662.872 | 1060.33 | 2.7 | 0.0603 | 1.536 |
| 8 | 50 | 6 | .0594 | 5.94 | 1:100 | - | 25 | 360.023 | 1060.33 | 2.7 | 6.0313 | 1.536 |
| | 51 | 6 | .0594 | 5.94 | 1:100 | - | 35 | 365.593 | 1060.33 | 2.69 | 6.0089 | 1.160 |
| | 52 | 6 | .0594 | 5.94 | 1:100 | - | 45 | 372.341 | 1060.33 | 2.65 | 5.9195 | 0.344 |
| | 53 | 6 | .0594 | 5.94 | 1:100 | - | 55 | 381.235 | 1060.33 | 2.67 | 5.9642 | 0.408 |
| | 54 | 6 | .0594 | 5.94 | 1:100 | - | 60 | 383.689 | 1060.33 | 2.67 | 5.9642 | 0.408 |
| | 55 | 6 | .0594 | 5.94 | 1:100 | - | 65 | 386.756 | 1060.33 | 2.7 | 6.0313 | 1.536 |
| | 56 | 6 | .0594 | 5.94 | 1:100 | - | 70 | 390.437 | 1060.33 | 2.65 | 5.9195 | 0.344 |
| 9 | 57 | 6 | 1 | 5 | 1:5 | - | 25 | 436.136 | 1060.33 | 2.22 | 4.9546 | 0.909 |
| | 58 | 6 | 1 | 5 | 1:5 | - | 35 | 443.497 | 1060.33 | 2.3 | 5.1378 | 2.755 |
| | 59 | 6 | 1 | 5 | 1:5 | - | 45 | 454.945 | 1060.33 | 2.25 | 5.0260 | 0.521 |
| | 60 | 6 | 1 | 5 | 1:5 | - | 55 | 465.886 | 1060.33 | 2.35 | 5.2830 | 4.989 |
| | 61 | 6 | 1 | 5 | 1:5 | - | 60 | 470.794 | 1060.33 | 2.3 | 5.1378 | 2.755 |
| | 62 | 6 | 1 | 5 | 1:5 | - | 65 | 476.621 | 1060.33 | 2.25 | 5.0260 | 0.521 |
| | 63 | 6 | 1 | 5 | 1:5 | - | 70 | 482.142 | 1060.33 | 2.3 | 5.1378 | 2.755 |

***Table A - 3 Results of the potentiometric titration of Fe(II) with Ce(IV) in the $H_2SO_4$-$Cu(SO_2)_4$-$Fe_2(SO_4)_3$-$FeSO_4$-$H_2O$ synthetic solution with a total of 6 g/L Iron.***

| Chemical Analysis | | Experimental results measured in the lab | | | | | | | | Calculated $Fe^{2+}$ amount by | | |
|---|---|---|---|---|---|---|---|---|---|---|---|---|
| Test | Assay | $Fe_{total}$ g/L | $Fe^{3+}$ g/L | $Fe^{2+}$ g/L | $Fe^{3+}/Fe^{2+}$ Nominal | $Cu^{2+}$ g/L | T ℃ | $E_b$ (obs) mV | $E_{End}$ (End) mV | ΔV ml | V (Calc) ml | Error % |
| 10 | 64 | 6 | 4 | 2 | 2:1 | 36 | 25 | 495.944 | 1060.33 | 9.1 | 2.0328 | 1.638 |
| | 65 | 6 | 4 | 2 | 2:1 | 36 | 35 | 506.372 | 1060.33 | 9.1 | 2.0329 | 1.638 |
| | 66 | 6 | 4 | 2 | 2:1 | 36 | 45 | 518.026 | 1060.33 | 9.2 | 2.0551 | 2.755 |
| | 67 | 6 | 4 | 2 | 2:1 | 36 | 55 | 531.215 | 1060.33 | 9.2 | 2.0551 | 2.755 |
| | 68 | 6 | 4 | 2 | 2:1 | 36 | 60 | 535.202 | 1060.33 | 9.2 | 2.0551 | 2.755 |
| | 69 | 6 | 4 | 2 | 2:1 | 36 | 65 | 541.643 | 1060.33 | 9.2 | 2.0551 | 2.755 |
| | 70 | 6 | 4 | 2 | 2:1 | 36 | 70 | 548.39 | 1060.33 | 9.15 | 2.0440 | 2.196 |
| 11 | 71 | 2.4 | 2 | 0.4 | 5:1 | 36 | 25 | 519.56 | 1060.33 | 1.75 | 0.3909 | 2.271 |
| | 72 | 2.4 | 2 | 0.4 | 5:1 | 36 | 35 | 530.908 | 1060.33 | 1.7 | 0.3798 | 5.064 |
| | 73 | 2.4 | 2 | 0.4 | 5:1 | 36 | 45 | 543.176 | 1060.33 | 1.8 | 0.4021 | 0.521 |
| | 74 | 2.4 | 2 | 0.4 | 5:1 | 36 | 55 | 556.068 | 1060.33 | 1.7 | 0.3798 | 5.064 |
| | 75 | 2.4 | 2 | 0.4 | 5:1 | 36 | 60 | 561.272 | 1060.33 | 1.8 | 0.4021 | 0.521 |
| | 76 | 2.4 | 2 | 0.4 | 5:1 | 36 | 65 | 567.713 | 1060.33 | 1.75 | 0.3909 | 2.271 |
| | 77 | 2.4 | 2 | 0.4 | 5:1 | 36 | 70 | 575.381 | 1060.33 | 1.7 | 0.3798 | 5.064 |
| 12 | 78 | 2.2 | 2 | 0.2 | 10:1 | 40 | 25 | 533.668 | 1060.33 | 9.5 | 0.2122 | 6.105 |
| | 79 | 2.2 | 2 | 0.2 | 10:1 | 40 | 35 | 545.63 | 1060.33 | 9.5 | 0.2122 | 6.105 |
| | 80 | 2.2 | 2 | 0.2 | 10:1 | 40 | 45 | 559.86 | 1060.33 | 9.5 | 0.2122 | 6.105 |
| | 81 | 2.2 | 2 | 0.2 | 10:1 | 40 | 55 | 572.313 | 1060.33 | 10 | 0.2234 | 11.69 |
| | 82 | 2.2 | 2 | 0.2 | 10:1 | 40 | 60 | 579.981 | 1060.33 | 10 | 0.2234 | 11.69 |
| | 83 | 2.2 | 2 | 0.2 | 10:1 | 40 | 65 | 585.809 | 1060.33 | 9 | 0.2010 | 0.521 |
| | 84 | 2.2 | 2 | 0.2 | 10:1 | 40 | 70 | 592.863 | 1060.33 | 10 | 0.2234 | 11.609 |
| 13 | 85 | 3 | 0.5 | 2.5 | 1:5 | 40 | 25 | 438.9 | 1060.33 | 11.3 | 2.5242 | 0.968 |
| | 86 | 3 | 0.5 | 2.5 | 1:5 | 40 | 35 | 448.4 | 1060.33 | 11.5 | 2.5689 | 0.968 |
| | 87 | 3 | 0.5 | 2.5 | 1:5 | 40 | 45 | 455.765 | 1060.33 | 11.3 | 2.5242 | 0.968 |
| | 88 | 3 | 0.5 | 2.5 | 1:5 | 40 | 55 | 465.886 | 1060.33 | 11.5 | 2.5689 | 2.755 |
| | 89 | 3 | 0.5 | 2.5 | 1:5 | 40 | 60 | 470.18 | 1060.33 | 11.3 | 2.5242 | 0.968 |
| | 90 | 3 | 0.5 | 2.5 | 1:5 | 40 | 65 | 476.928 | 1060.33 | 11.3 | 2.5242 | 0.968 |
| | 91 | 3 | 0.5 | 2.5 | 1:5 | 40 | 70 | 481.835 | 1060.33 | 11.5 | 2.5689 | 2.755 |
| 14 | 92 | 6 | 5.459 | 0.545 | 10:1 | 45 | 25 | 536.736 | 1060.33 | 2.5 | 0.5585 | 2.468 |
| | 93 | 6 | 5.459 | 0.545 | 10:1 | 45 | 35 | 545.323 | 1060.33 | 2.55 | 0.5696 | 4.517 |
| | 94 | 6 | 5.459 | 0.545 | 10:1 | 45 | 45 | 560.659 | 1060.33 | 2.5 | 0.5585 | 2.468 |
| | 95 | 6 | 5.459 | 0.545 | 10:1 | 45 | 55 | 574.154 | 1060.33 | 2.5 | 0.5585 | 2.468 |
| | 96 | 6 | 5.459 | 0.545 | 10:1 | 45 | 60 | 579.981 | 1060.33 | 2.55 | 0.5696 | 4.517 |
| | 97 | 6 | 5.459 | 0.545 | 10:1 | 45 | 65 | 586.115 | 1060.33 | 2.55 | 0.5696 | 4.517 |
| | 98 | 6 | 5.459 | 0.545 | 10:1 | 45 | 70 | 593.476 | 1060.33 | 2.5 | 0.5585 | 2.468 |
| 15 | 99 | 3 | 2 | 1 | 2:1 | 45 | 25 | 495.33 | 1060.33 | 4.6 | 1.0275 | 2.755 |
| | 100 | 3 | 2 | 1 | 2:1 | 45 | 35 | 503.918 | 1060.33 | 4.6 | 1.0275 | 2.755 |
| | 101 | 3 | 2 | 1 | 2:1 | 45 | 45 | 515.573 | 1060.33 | 4.55 | 1.0164 | 1.638 |
| | 102 | 3 | 2 | 1 | 2:1 | 45 | 55 | 528.148 | 1060.33 | 4.6 | 1.0275 | 2.755 |
| | 103 | 3 | 2 | 1 | 2:1 | 45 | 60 | 534.282 | 1060.33 | 4.6 | 1.0275 | 2.755 |
| | 104 | 3 | 2 | 1 | 2:1 | 45 | 65 | 540.416 | 1060.33 | 4.5 | 1.0052 | 0.521 |
| | 105 | 3 | 2 | 1 | 2:1 | 45 | 70 | 547.164 | 1060.33 | 4.55 | 1.0164 | 1.638 |
| 16 | 106 | 3 | 2 | 1 | 2:1 | 50 | 25 | 497.17 | 1060.33 | 4.7 | 1.0499 | 4.989 |
| | 107 | 3 | 2 | 1 | 2:1 | 50 | 35 | 506.065 | 1060.33 | 4.65 | 1.0387 | 3.872 |
| | 108 | 3 | 2 | 1 | 2:1 | 50 | 45 | 517.72 | 1060.33 | 4.7 | 1.0499 | 4.989 |
| | 109 | 3 | 2 | 1 | 2:1 | 50 | 55 | 530.295 | 1060.33 | 4.7 | 1.0499 | 4.989 |
| | 110 | 3 | 2 | 1 | 2:1 | 50 | 60 | 535.202 | 1060.33 | 4.7 | 1.0499 | 4.989 |
| | 111 | 3 | 2 | 1 | 2:1 | 50 | 65 | 541.95 | 1060.33 | 4.65 | 1.0387 | 3.872 |
| | 112 | 3 | 2 | 1 | 2:1 | 50 | 70 | 548.084 | 1060.33 | 4.5 | 1.0052 | 0.521 |

Vita

Daniel Pedro Cruz was born and raised in El Paso, Texas. He attended The University of Texas at El Paso, where he earned a Bachelor of Science in Metallurgical and Materials Engineering in 2007. He began work on his Master of Science in Metallurgical and Materials Engineering in 2017, focusing on hydrometallurgical processes.

While at The University of Texas at El Paso, Daniel was elected President of the Society of Mining, Metallurgy & Exploration, and served on several associations including the Alpha Sigma Mu Honor Society and Material Advantage Society. Daniel also developed as a peer advisor for the College of Engineering.

Currently, Daniel is a Metallurgist at Freeport-McMoRan Inc. in Bagdad, Arizona, Living in Bagdad, Arizona.